

# Physics of Spin Hall Effect

**Guang-Yu Guo (郭光宇)**

**Physics Dept, National Taiwan University, Taiwan**

**(國立臺灣大學物理系)**

**(A Talk in Institute for Advanced Studies,**

**Tsinghua University, Beijing, 11 Sept. 2013)**

# Plan of this Talk

## I. Introduction

1. Spin Hall effect.
2. Motivations.

## II. Intrinsic spin Hall effect in solids

1. Berry phase formalism for intrinsic Hall effects.
2. Large intrinsic spin Hall effect in platinum
3. Intrinsic spin Hall effect in other pure  $4d$  and  $5d$  metals

## III. Gigantic spin Hall effect in gold and multi-orbital Kondo effect

1. Gigantic spin Hall effect in gold/FePt
2. Multi-orbital Kondo effect in Fe impurity in gold.
3. Enhanced spin Hall effect by resonant skew scattering in orbital-dependent Kondo effect.
4. Quantum Monte Carlo simulation
5. Open questions

## IV. Summary

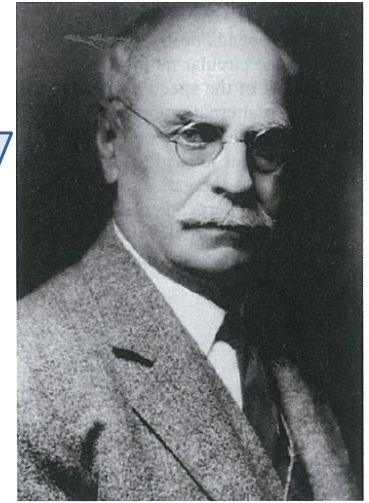
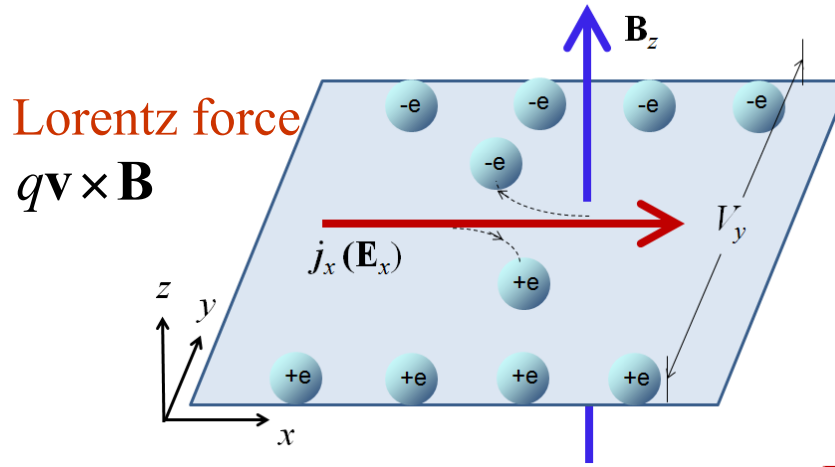
# I. Introduction

## 1. Spin Hall effect

### 1) Ordinal Hall Effect

[Hall 1879]

$$\rho_{\text{Hall}} = R_0 B$$



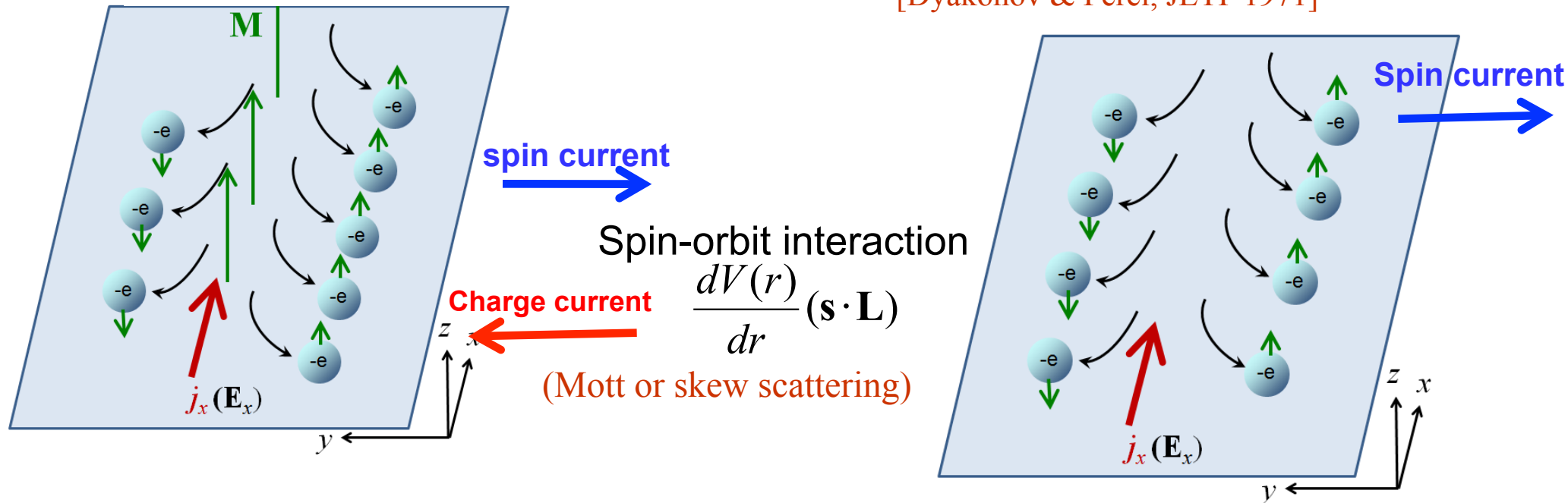
Edwin H. Hall (1855-1938)

### 2) Anomalous Hall Effect [Hall, 1880 & 1881]

$$\rho_{\text{Hall}} = R_0 B + R_S M$$

### 3) (extrinsic) Spin Hall Effect

[Dyakonov & Perel, JETP 1971]



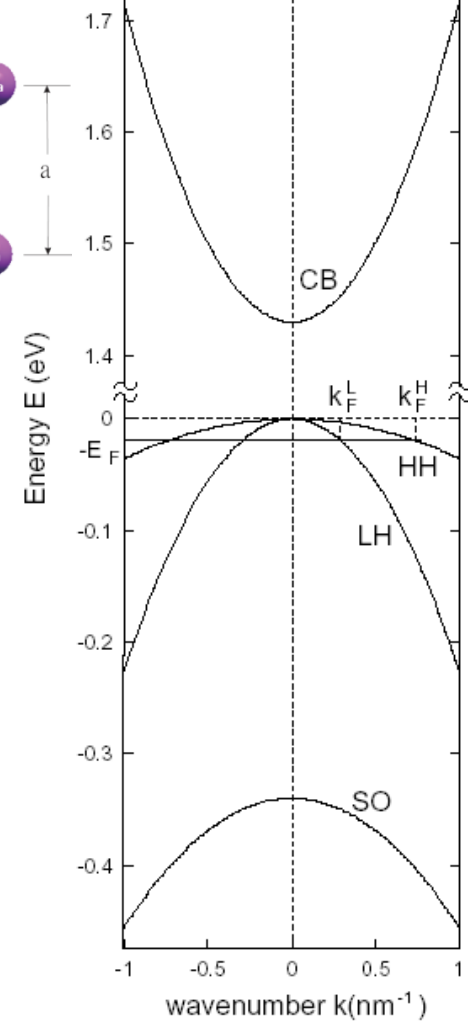
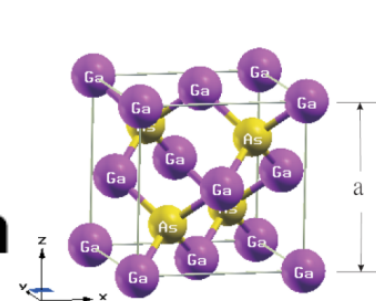
# 4) Intrinsic spin Hall effect

## (1) In p-type zincblende semiconductors

# Dissipationless Quantum Spin Current at Room Temperature

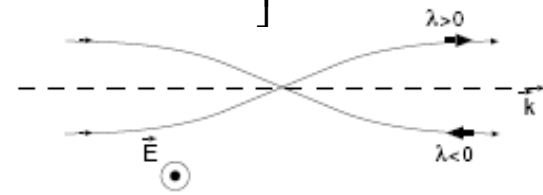
Shuichi Murakami,<sup>1\*</sup> Naoto Nagaosa,<sup>1,2,3</sup> Shou-Cheng Zhang<sup>4</sup>

5 SEPTEMBER 2003 VOL 301 SCIENCE www.sciencemag.org



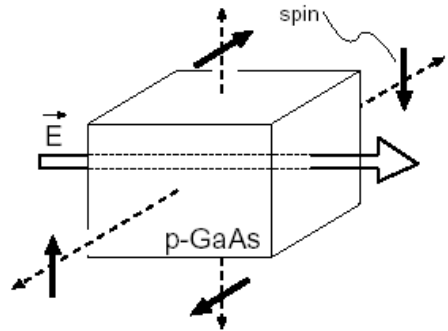
Luttinger model 
$$H_0 = \frac{\hbar^2}{2m} \left[ \left( \gamma_1 + \frac{5}{2} \gamma_2 \right) k^2 - 2\gamma_2 (\vec{k} \cdot \vec{S})^2 \right]$$

Equation of motion 
$$\langle \dot{X}_i \rangle = \frac{\hbar k_i}{m_\lambda} + F_{il} \langle \dot{k}_l \rangle$$



$$\langle \dot{k}_i \rangle = \frac{e}{\hbar} E_i \quad e > 0 \text{ (hole)}$$

Anomalous velocity 
$$\langle \dot{X} \rangle = \frac{\hbar \vec{k}}{m_\lambda} - \frac{e\lambda}{\hbar k^3} \vec{k} \times \vec{E}$$



$$j_j^i = \sigma_s \epsilon^{ijk} E_k \quad (1)$$

$$j_y^x = \frac{eE_z}{12\pi^2} (3k_F^H - k_F^L) = \frac{\hbar}{2e} \sigma_s E_z \quad (10)$$

$n_h = 10^{19} \text{ cm}^{-3}$ ,  $\mu = 50 \text{ cm}^2/\text{V}\cdot\text{s}$ ,  $\sigma = e\mu n_h = 80 \text{ } \Omega^{-1}\text{cm}^{-1}$ ;  
 $\sigma_s = 80 \text{ } \Omega^{-1}\text{cm}^{-1}$   
 $n_h = 10^{16} \text{ cm}^{-3}$ ,  $\mu = 50 \text{ cm}^2/\text{V}\cdot\text{s}$ ,  $\sigma = e\mu n_h = 0.6 \text{ } \Omega^{-1}\text{cm}^{-1}$ ;  
 $\sigma_s = 7 \text{ } \Omega^{-1}\text{cm}^{-1}$

## (2) In a 2-D electron gas in n-type semiconductor heterostructures Universal Intrinsic Spin Hall Effect

Jairo Sinova,<sup>1,2</sup> Dimitrie Culcer,<sup>2</sup> Q. Niu,<sup>2</sup> N. A. Sinitsyn,<sup>1</sup> T. Jungwirth,<sup>2,3</sup> and A. H. MacDonald<sup>2</sup>

<sup>1</sup>Department of Physics, Texas A&M University, College Station, Texas 77843-4242, USA

<sup>2</sup>Department of Physics, University of Texas at Austin, Austin, Texas 78712-1081, USA

<sup>3</sup>Institute of Physics ASCR, Cukrovarnická 10, 162 53 Praha 6, Czech Republic

(Received 27 July 2003; published 25 March 2004)

### Rashba Hamiltonian

$$H = \frac{p^2}{2m} - \frac{\lambda}{\hbar} \vec{\sigma} \cdot (\hat{z} \times \vec{p}), \quad (1)$$

contributes to the spin current. In this case we find that the spin current in the  $\hat{y}$  direction is [23]

$$j_{s,y} = \int_{\text{annulus}} \frac{d^2\vec{p}}{(2\pi\hbar)^2} \frac{\hbar n_{z,\vec{p}} p_y}{2} \frac{p_y}{m} = \frac{-eE_x}{16\pi\lambda m} (p_{F+} - p_{F-}), \quad (6)$$

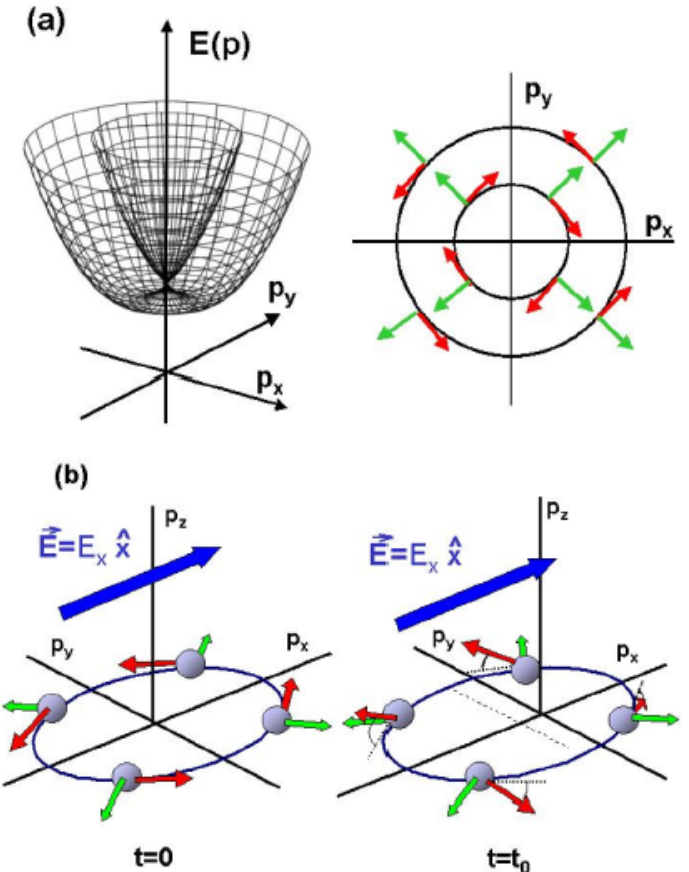
where  $p_{F+}$  and  $p_{F-}$  are the Fermi momenta of the majority and minority spin Rashba bands. We find that when both bands are occupied, i.e., when  $n_{2D} > m^2\lambda^2/\pi\hbar^4 \equiv n_{2D}^*$ ,  $p_{F+} - p_{F-} = 2m\lambda/\hbar$  and then the spin Hall (SH) conductivity is

### Universal spin Hall conductivity

$$\sigma_{\text{SH}} \equiv -\frac{j_{s,y}}{E_x} = \frac{e}{8\pi}, \quad (7)$$

independent of both the Rashba coupling strength and of the 2DES density. For  $n_{2D} < n_{2D}^*$  the upper Rashba band is depopulated. In this limit  $p_{F-}$  and  $p_{F+}$  are the interior and exterior Fermi radii of the lowest Rashba split band, and  $\sigma_{\text{SH}}$  vanishes linearly with the 2DES density:

$$\sigma_{\text{SH}} = \frac{e}{8\pi} \frac{n_{2D}}{n_{2D}^*}. \quad (8)$$



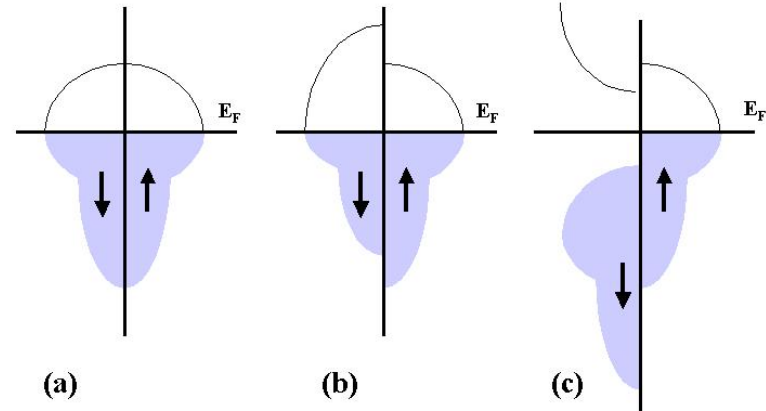
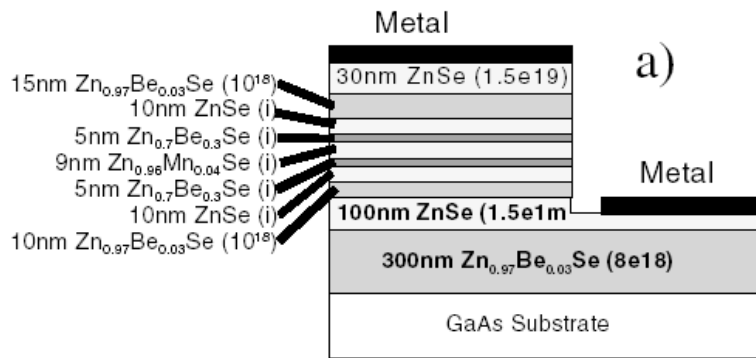
### (3) Significances of these theoretical discoveries of intrinsic spin Hall effects

Basic elements of spintronics (spin electronics):

Generation, detection, & manipulation of spin current.

Usual spin current generations:

Ferromagnetic leads



(a) non-magnetic metals, (b) ferromagnetic metals and (c) half-metallic metals.

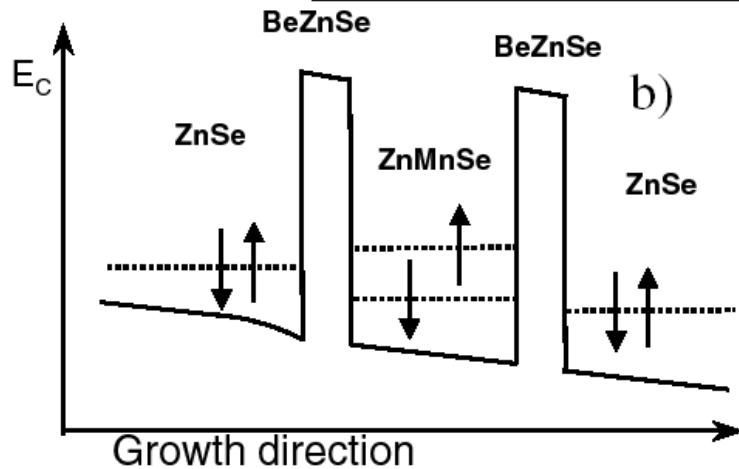


FIG. 1. (a) Layer structure of the device and (b) schematic view of resonant tunnel diode band structure under bias.

Spin filter

[Slobodskyy, et al., PRL 2003]

Problems: magnets and/or magnetic fields needed, and difficult to integrate with semiconductor technologies.

It would allow to generate spin current electrically in semiconductor microstructures without applied magnetic fields or magnetic materials, and make possible pure electric driven spintronics which could be readily integrated with conventional electronics.

# 5) Experiments on spin Hall effect in semiconductors

(a) in n-type 3D GaAs and InGaAs thin films [Kato *et al.*, Science 306, 1910 (2004)]

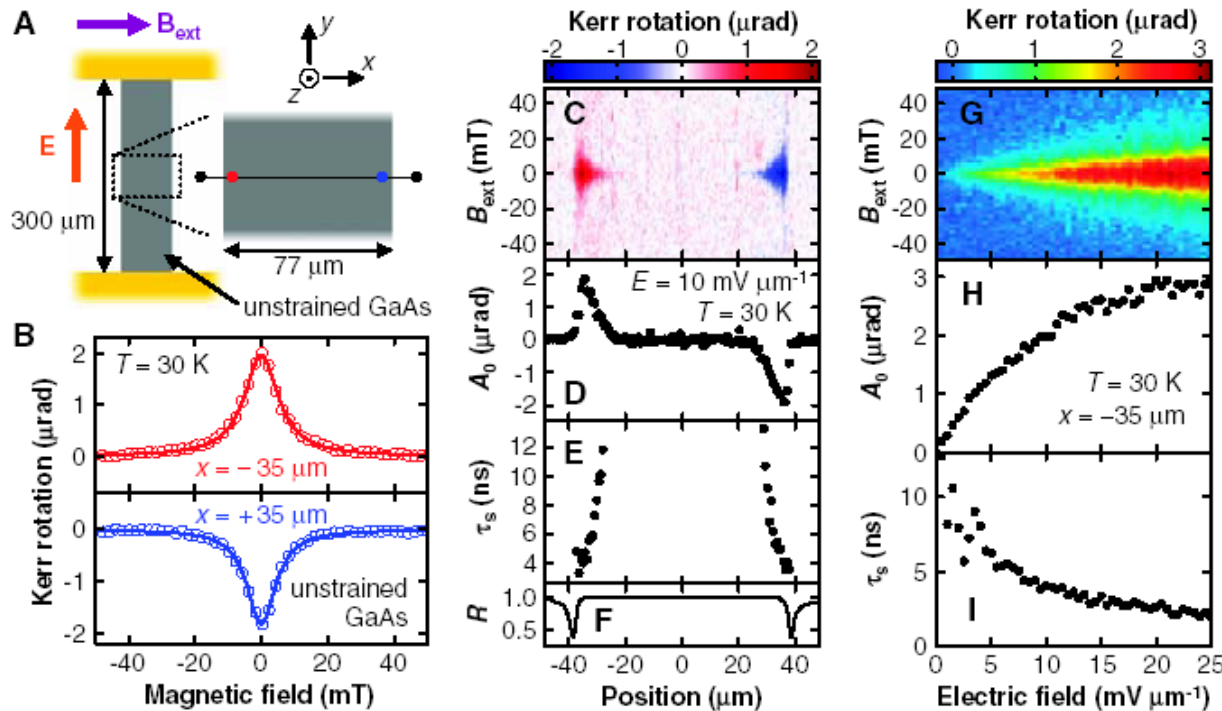


**Fig. 1.** The spin Hall effect in unstrained GaAs. Data are taken at  $T = 30$  K; a linear background has been subtracted from each  $B_{\text{ext}}$  scan. (A) Schematic of the unstrained GaAs sample and the experimental geometry. (B) Typical measurement of KR as a function of  $B_{\text{ext}}$  for  $x = -35 \mu\text{m}$  (red circles) and  $x = +35 \mu\text{m}$  (blue circles) for  $E = 10 \text{ mV } \mu\text{m}^{-1}$ . Solid lines are fits as explained in text. (C) KR as a function of  $x$  and  $B_{\text{ext}}$  for  $E = 10 \text{ mV } \mu\text{m}^{-1}$ . (D and E) Spatial dependence of peak KR  $A_0$  and spin lifetime  $\tau_s$  across the channel, respectively, obtained from fits to data in (C). (F) Reflectivity  $R$  as a function of  $x$ .  $R$  is normalized to the value on the GaAs channel. The two dips indicate the position of the edges and the width of the dips gives an approximate spatial resolution. (G) KR as a function of  $E$  and  $B_{\text{ext}}$  at  $x = -35 \mu\text{m}$ . (H and I)  $E$  dependence of  $A_0$  and  $\tau_s$ , respectively, obtained from fits to data in (G).

Attributed to extrinsic SHE because of weak crystal direction dependence.

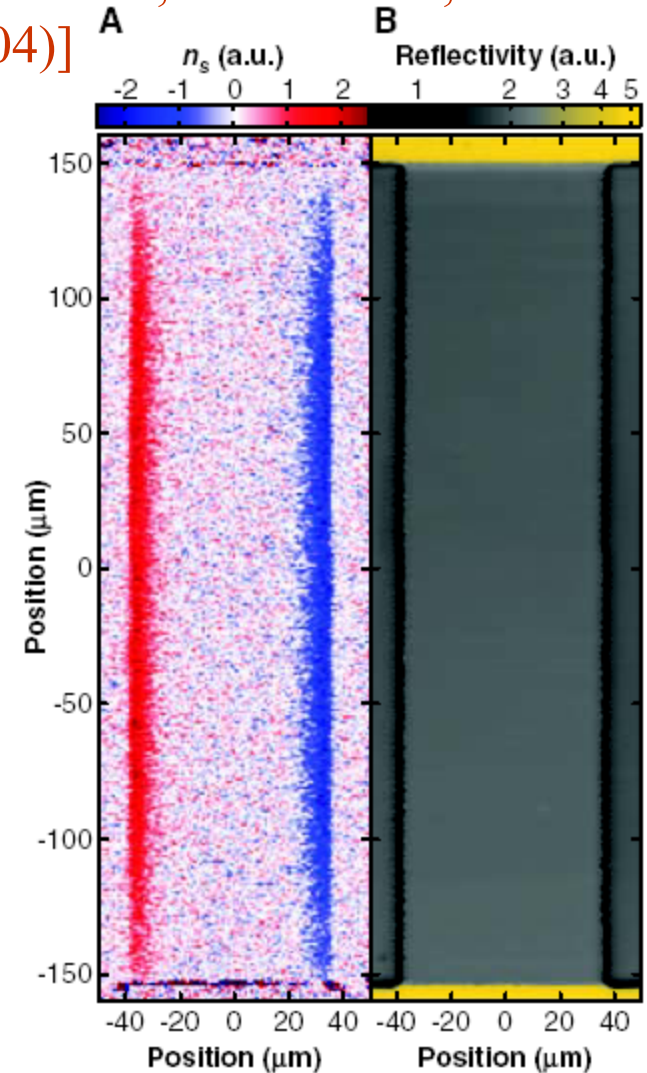


**Fig. 2.** (A and B) Two-dimensional images of spin density  $n_s$  and reflectivity  $R$ , respectively, for the unstrained GaAs sample measured at  $T = 30$  K and  $E = 10 \text{ mV } \mu\text{m}^{-1}$ .

## (b) in p-type 2D semiconductor quantum wells

### Experimental Observation of the Spin-Hall Effect in a Two-Dimensional Spin-Orbit Coupled Semiconductor System

J. Wunderlich,<sup>1</sup> B. Kaestner,<sup>1,2</sup> J. Sinova,<sup>3</sup> and T. Jungwirth<sup>4,5</sup>

<sup>1</sup>Hitachi Cambridge Laboratory, Cambridge CB3 0HE, United Kingdom

<sup>2</sup>National Physical Laboratory, Teddington T11 0LW, United Kingdom

<sup>3</sup>Department of Physics, Texas A&M University, College Station, Texas 77843-4242, USA

<sup>4</sup>Institute of Physics ASCR, Cukrovarnická 10, 162 53 Praha 6, Czech Republic

<sup>5</sup>School of Physics and Astronomy, University of Nottingham, Nottingham NG7 2RD, United Kingdom

(Received 16 November 2004; published 4 February 2005)

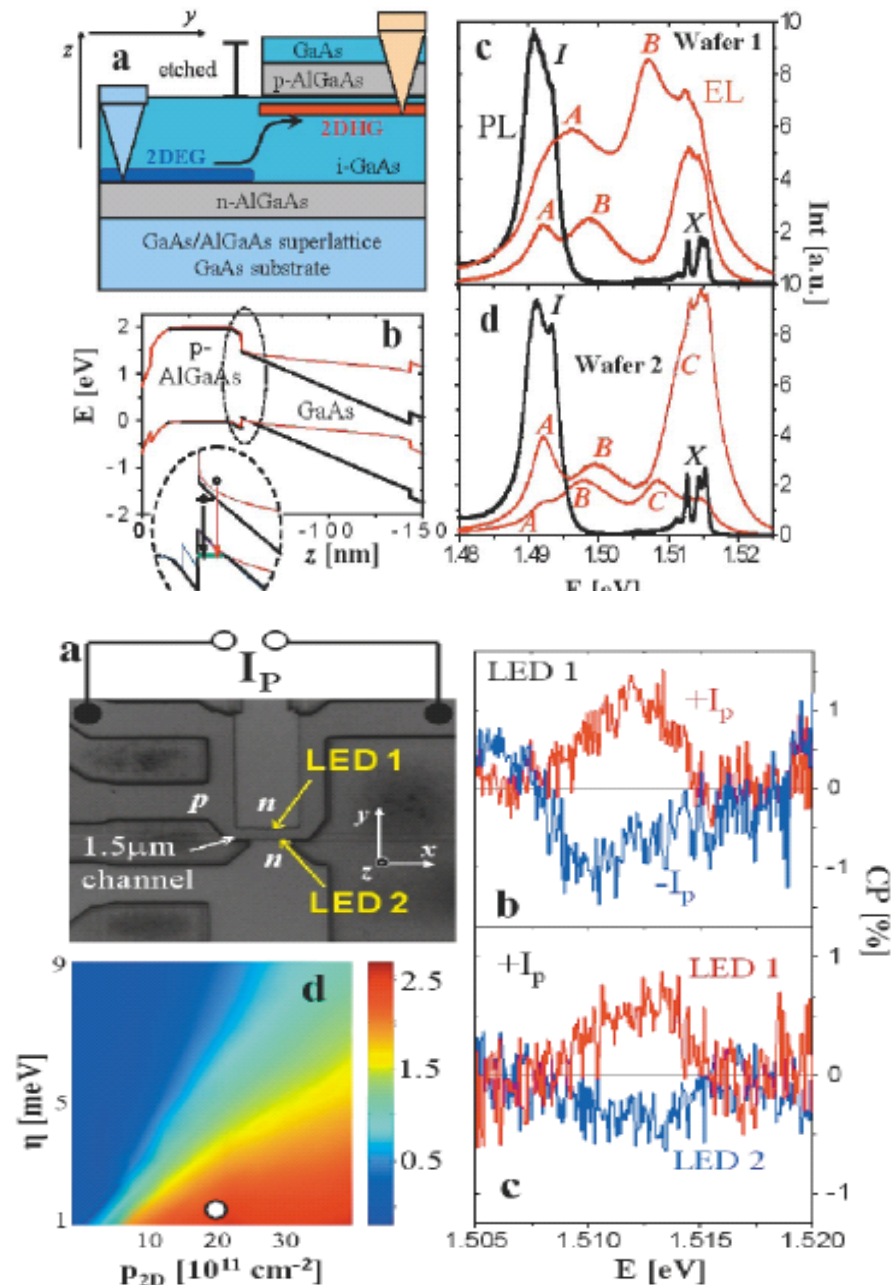
We report the experimental observation of the spin-Hall effect in a 2D hole system with spin-orbit coupling. The 2D hole layer is a part of a *p-n* junction light-emitting diode with a specially designed coplanar geometry which allows an angle-resolved polarization detection at opposite edges of the 2D hole system. In equilibrium the angular momenta of the spin-orbit split heavy-hole states lie in the plane of the 2D layer. When an electric field is applied across the hole channel, a nonzero out-of-plane component of the angular momentum is detected whose sign depends on the sign of the electric field and is opposite for the two edges. Microscopic quantum transport calculations show only a weak effect of disorder, suggesting that the clean limit spin-Hall conductance description (intrinsic spin-Hall effect) might apply to our system.

DOI: 10.1103/PhysRevLett.94.047204

PACS numbers: 75.50.Pp, 71.70.Ej, 85.75.Mm

[Wunderlich, et al., PRL 94 (2005) 047204]

Attributed to intrinsic SHE.





# 6) Spin Hall effect in metals

Nature 13 July 2006 Vol. 442, P. 04937

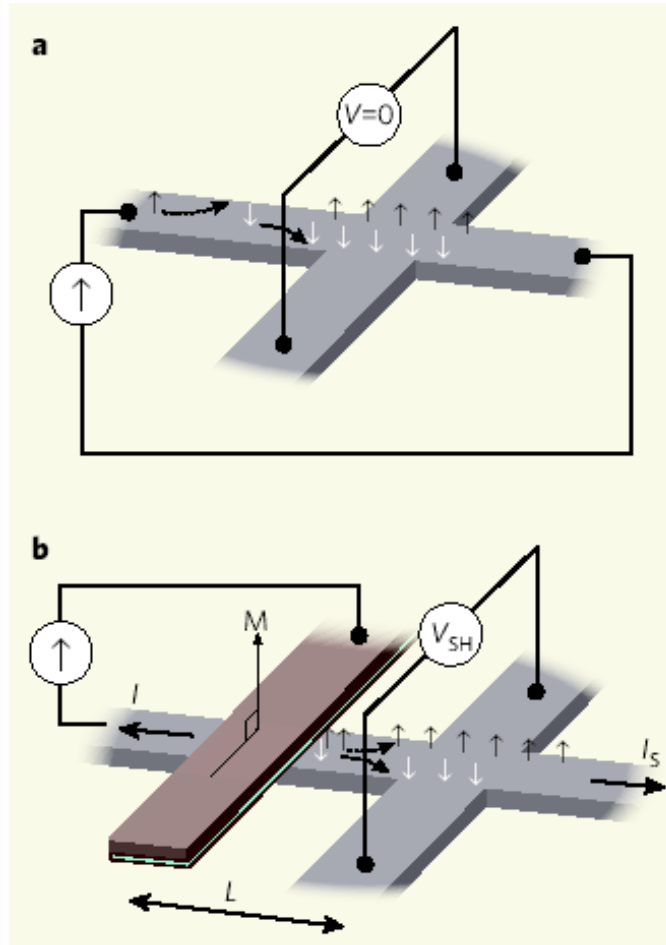
## Direct electronic measurement of the spin Hall effect

S. O. Valenzuela<sup>1</sup>† & M. Tinkham<sup>1</sup>

fcc Al

$$\sigma_{\text{SH}} = 27\sim 34 (\Omega\text{cm})^{-1}$$

( $T = 4.2 \text{ K}$ )



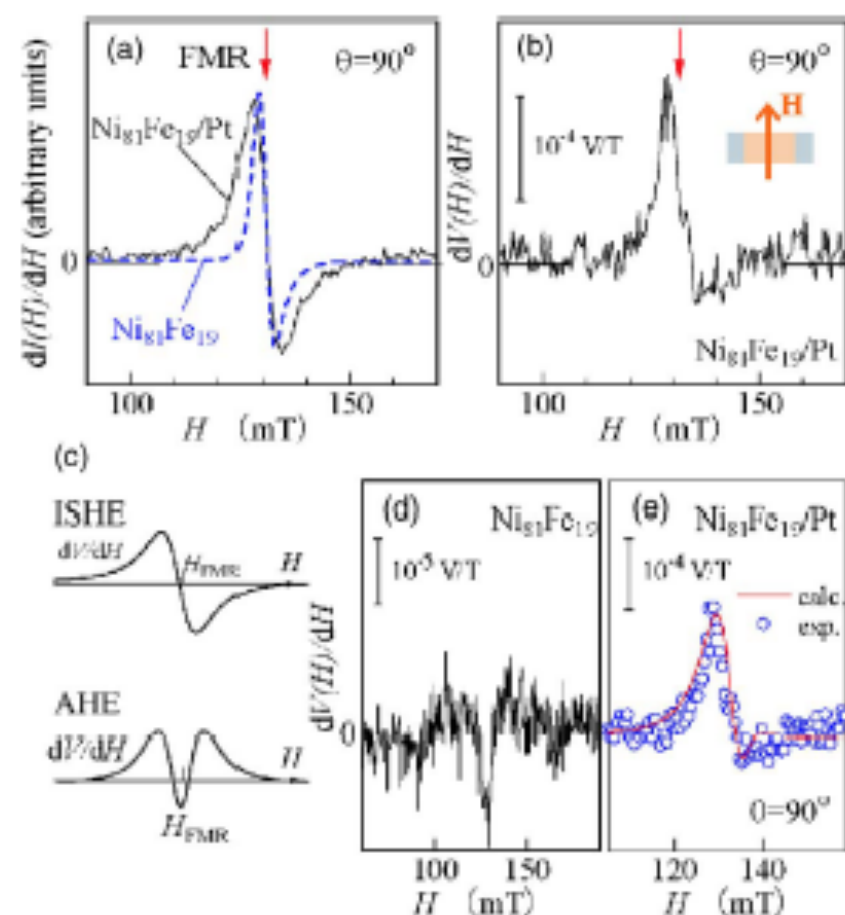
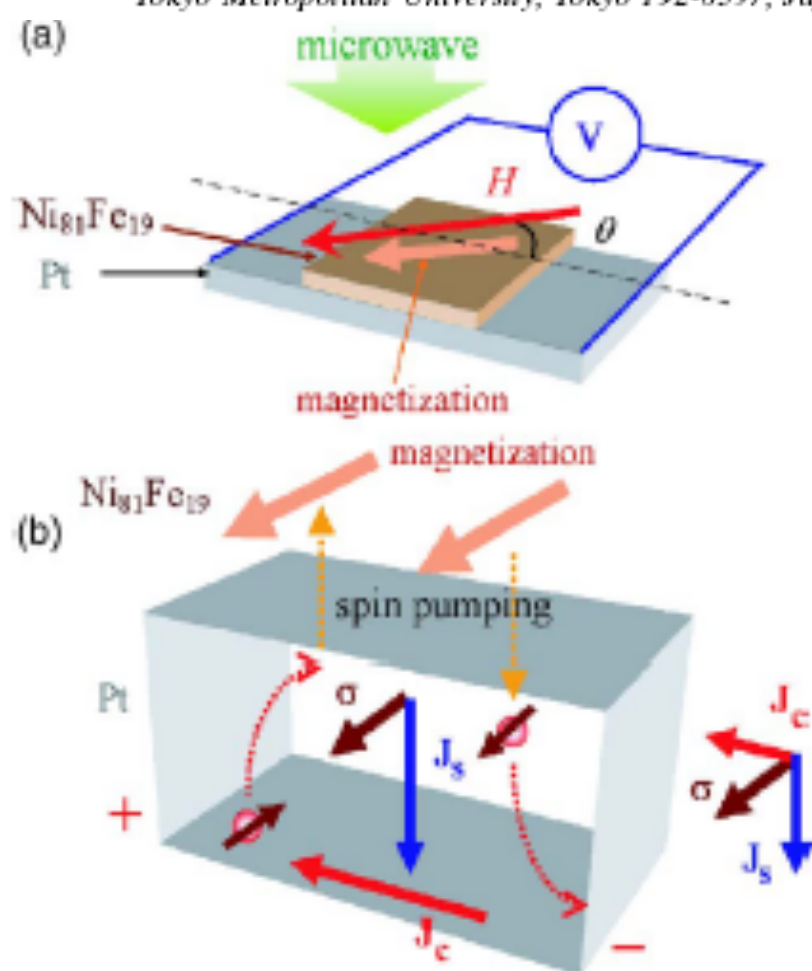
# Conversion of spin current into charge current at room temperature: Inverse spin-Hall effect

E. Saitoh,<sup>a)</sup> M. Ueda, and H. Miyajima

*Department of Physics, Keio University, Yokohama 223-8522, Japan*

G. Tatara

*PRESTO, Japan Science and Technology Agency (JST), Department of Physics,  
Tokyo Metropolitan University, Tokyo 192-0397, Japan*

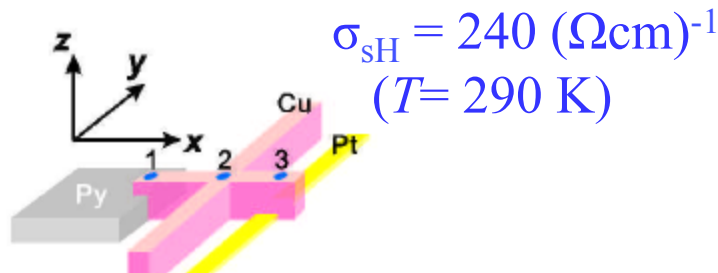
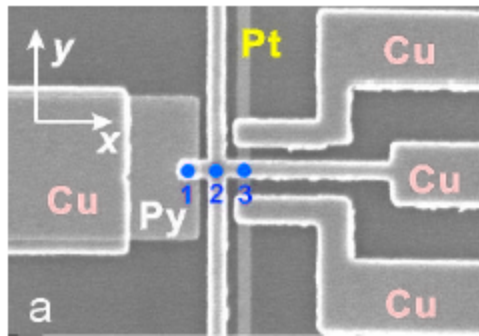


# Room Temperature Reversible Spin Hall Effect

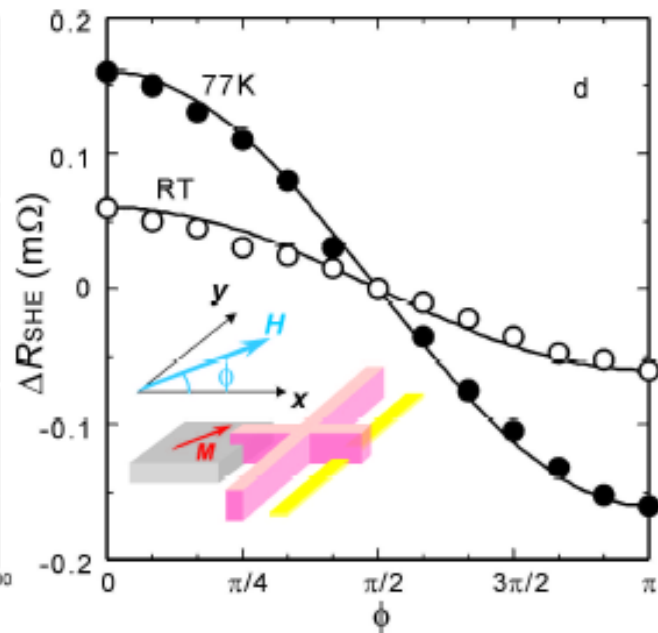
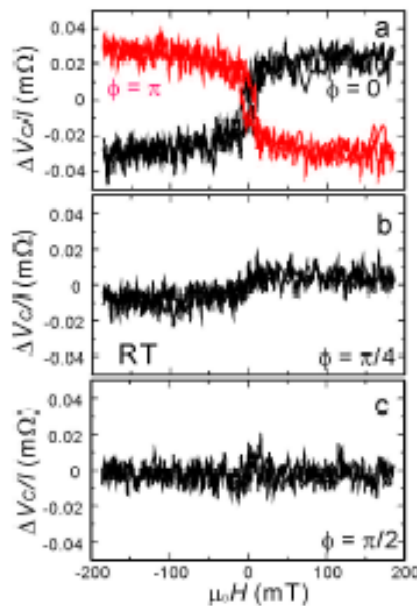
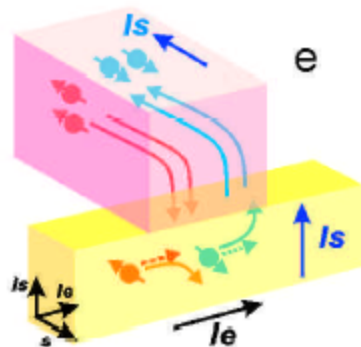
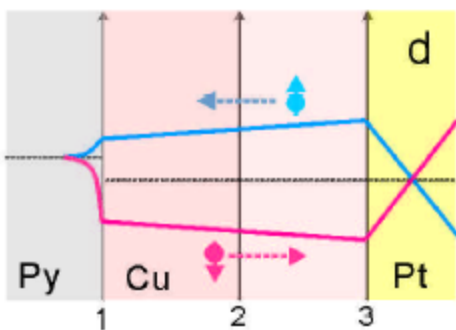
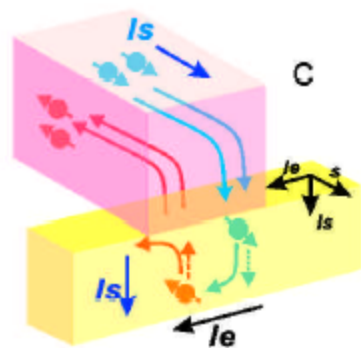
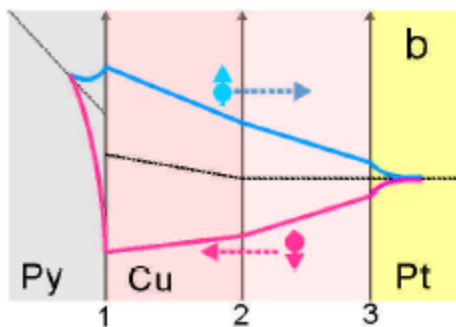
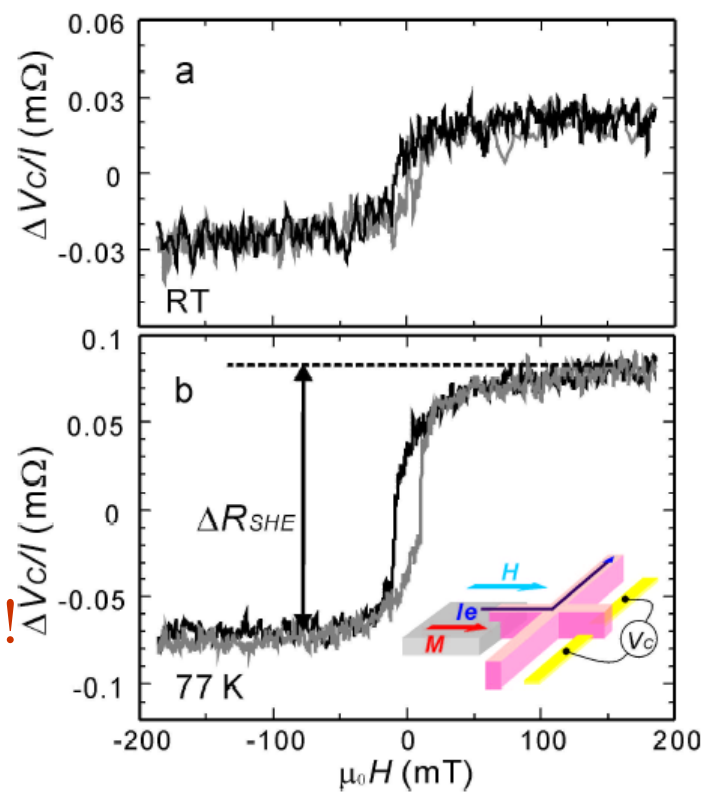
[PRL98, 156601; 98 (2007), 139901 (E) (2007)]

T. Kimura,<sup>1,2</sup> Y. Otani,<sup>1,2</sup> T. Sato,<sup>1</sup> S. Takahashi,<sup>3,4</sup> and S. Maekawa<sup>3,4</sup>

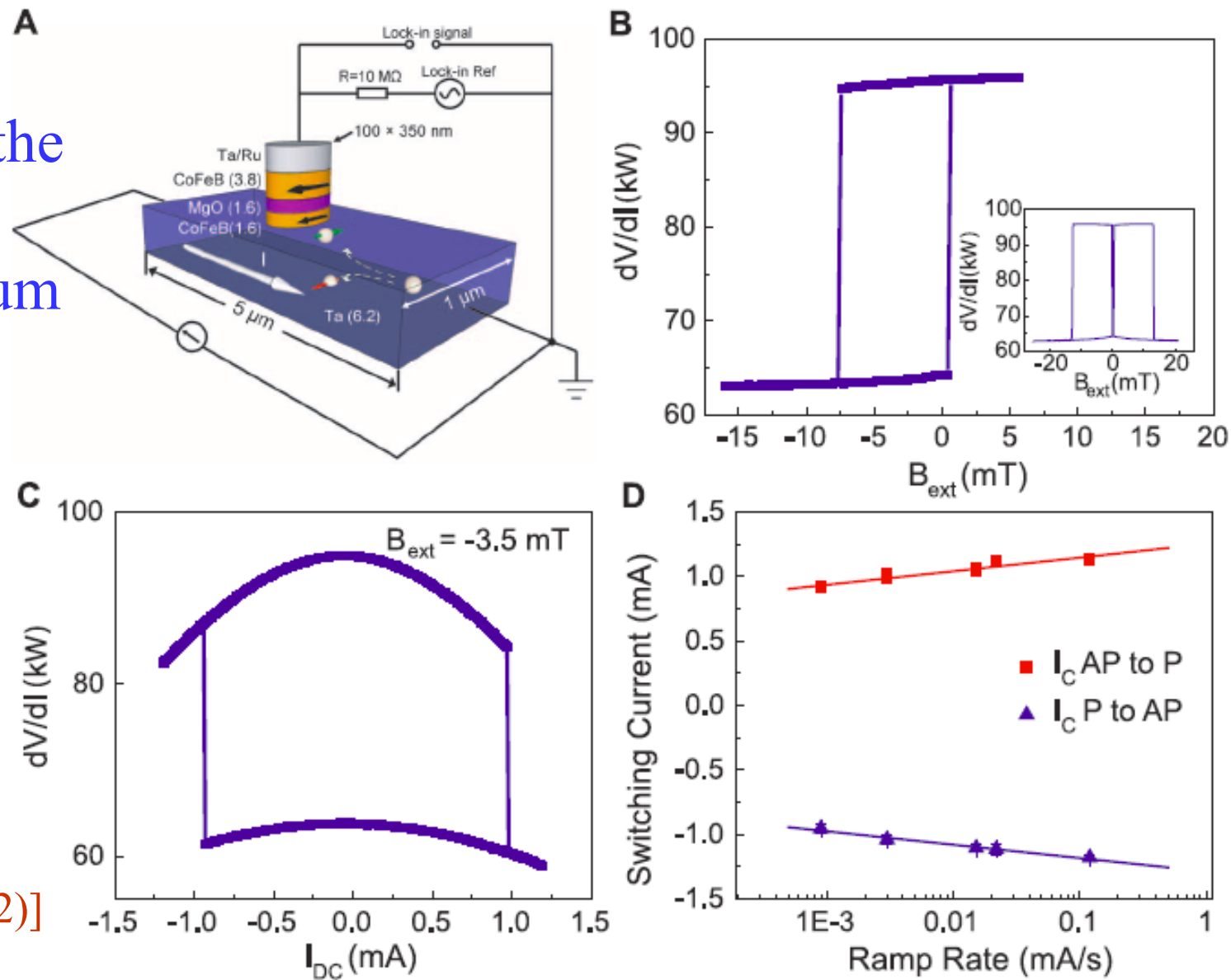
<sup>1</sup> Institute for Solid State Physics, University of Tokyo



Assumed to be extrinsic!



# Spin-Torque Switching with the Giant Spin Hall Effect of Tantalum



[L. Liu et al.,  
Science 336, 555 (2012)]

**Fig. 3.** Spin Hall effect-induced switching for an in-plane magnetized nanomagnet at room temperature. **(A)** Schematic of the three-terminal SHE devices and the circuit for measurements. The direction of the spin Hall spin transfer torque is not the same as in Fig. 1A because the CoFeB layer now lies above the Ta rather than below. **(B)** TMR minor loop of the MTJ as a function of the external applied field  $B_{ext}$  applied in-plane along the long axis of the sample. (Inset) TMR major loop of the device. **(C)**

## 2. Motivations

### 1) Questions on the intrinsic spin Hall effect in semiconductors?

(1) Will the intrinsic spin Hall effect exactly cancelled by the intrinsic orbital-angular-momentum Hall effect?

[S. Zhang and Z. Yang, cond-mat/0407704; PRL 2005]

In conclusion, we have shown that the ISHE is accompanied by the intrinsic orbital-angular-momentum Hall effect so that the total angular momentum spin current is zero in a SOC system.

For Rashba Hamiltonian, 
$$J_{int}^{spin} = \frac{e}{8\pi} E; \quad J_{int}^{orbit} = -\frac{e}{8\pi} E.$$

This is confirmed for Rashba system by us. However, in Dresselhaus and Rashba systems, spin Hall conductivity would not be cancelled by the orbital Hall conductivity.

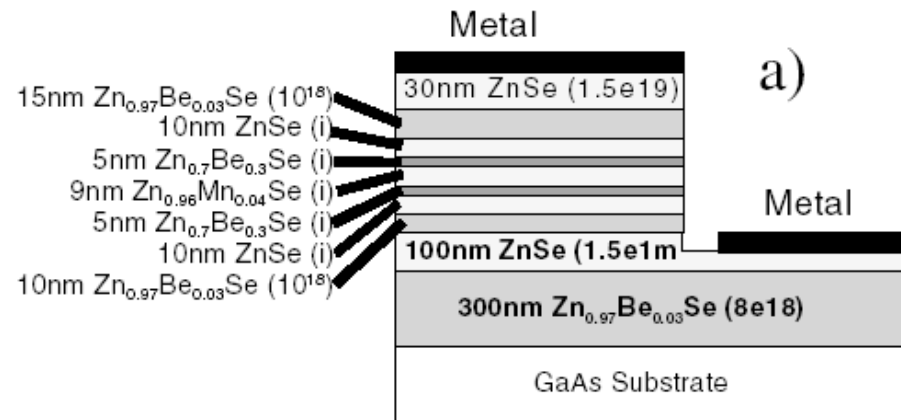
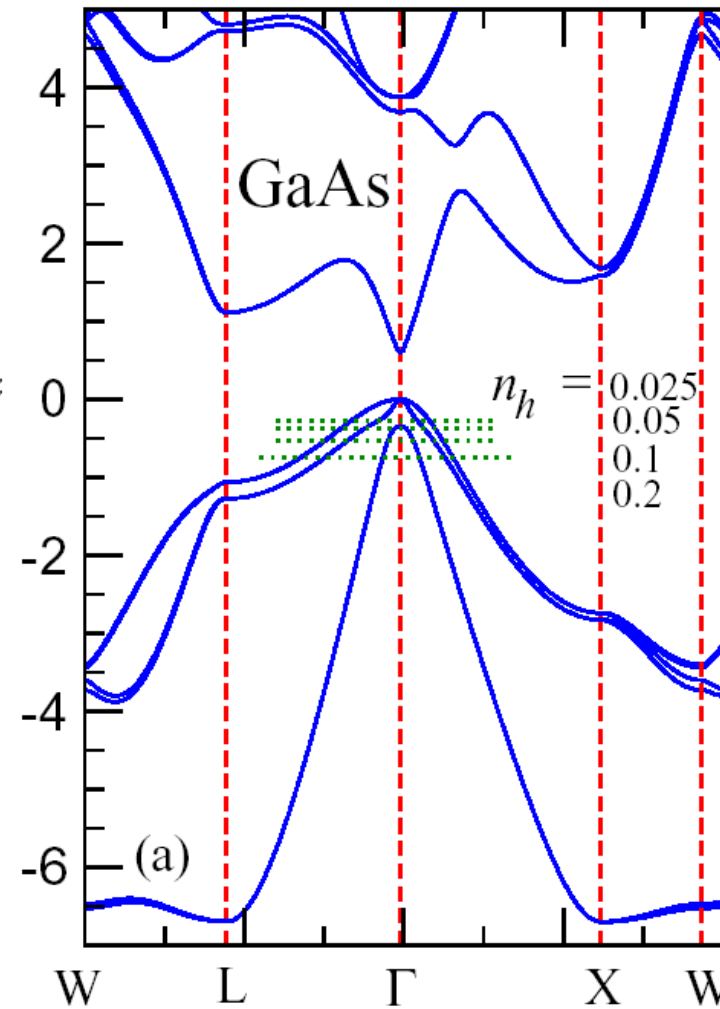
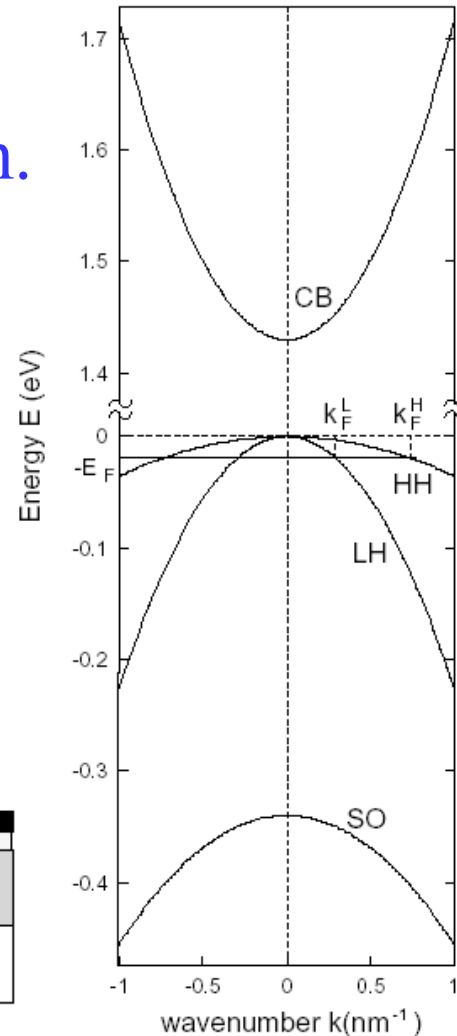
[Chen, Huang, Guo, PRB73 (2006) 235309]

## 2) Motivations

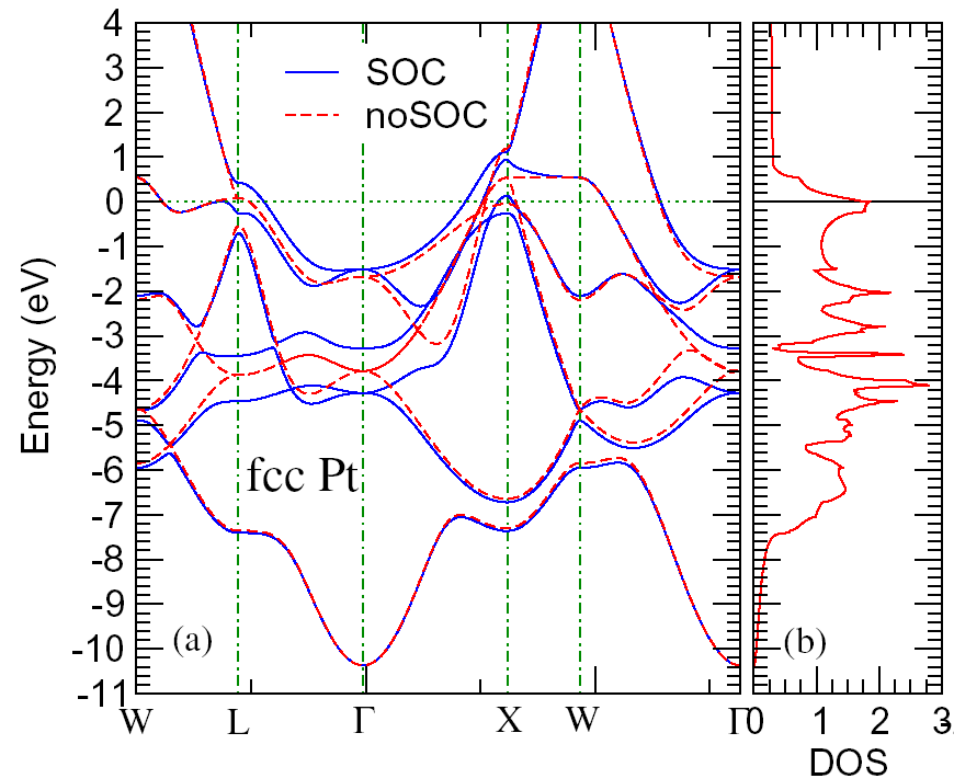
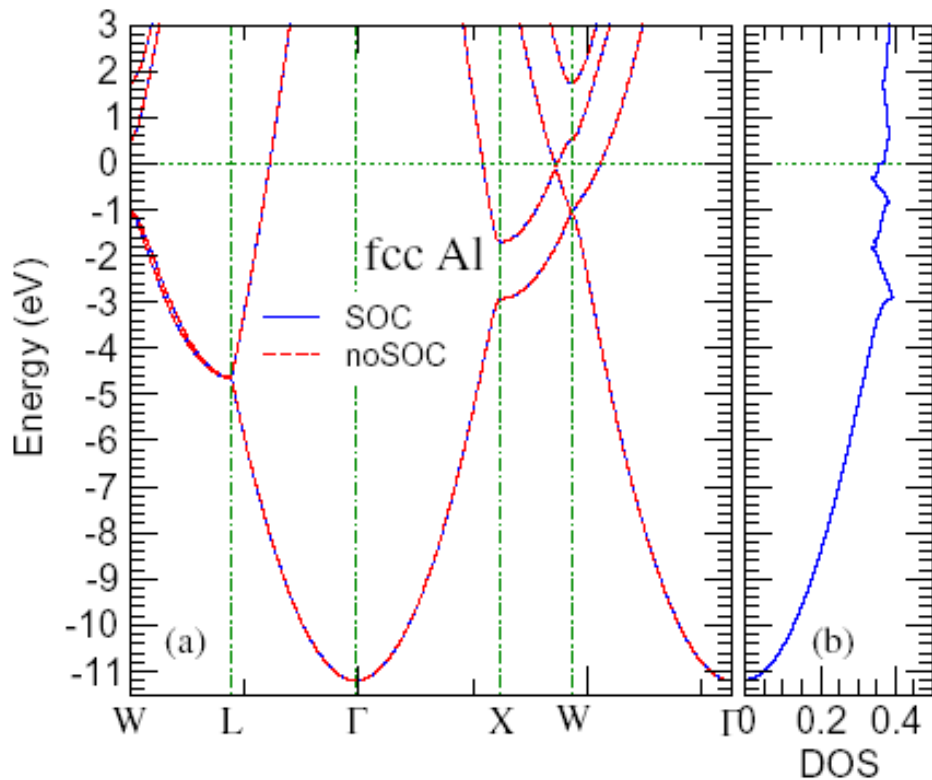
(1) Try to resolve the above important problem(s).

(2) To go beyond the spherical 4-band Luttinger Hamiltonian.

(3) To understand the effects of epitaxial strains.



(4) It is important to understand the detailed mechanism of the SHE in metals because it would lead to the material design of the large SHE even at room temperature with the application to the spintronics. To this end, *ab initio* band theoretical calculations for real metal systems is essential.



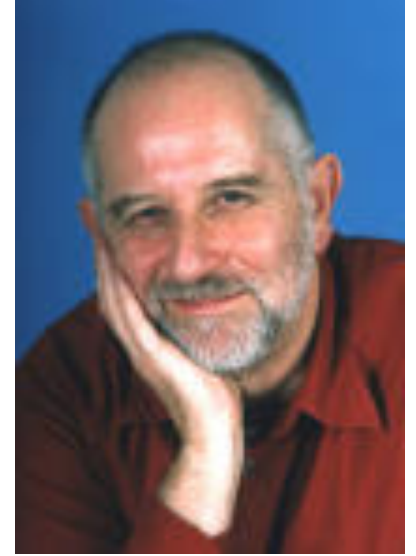
## II. Intrinsic spin Hall effect in solids

### 1. Berry phase formalism for intrinsic Hall effects

[Based on slides from Niu's talks]

#### (1) Berry phase

[Berry, Proc. Roy. Soc. London A 392, 451 (1984)]



Parameter dependent system:

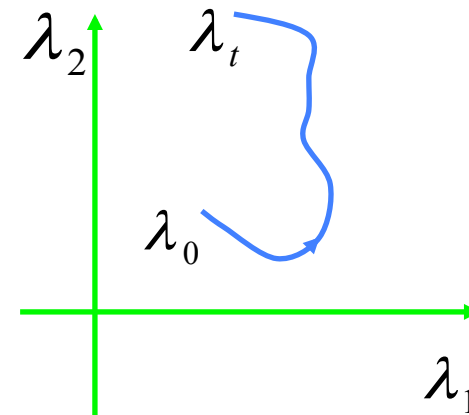
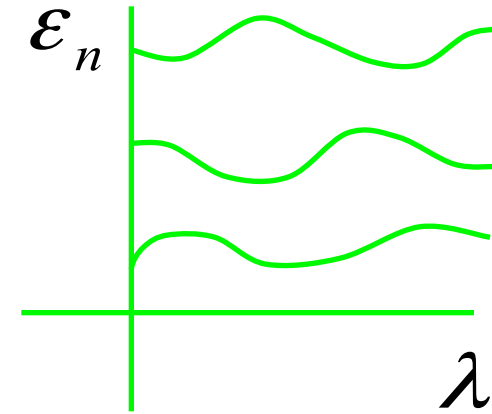
$$\{ \varepsilon_n(\lambda), \psi_n(\lambda) \}$$

Adiabatic theorem:

$$\Psi(t) = \psi_n(\lambda(t)) e^{-i \int_0^t dt \varepsilon_n / \hbar} e^{-i \gamma_n(t)}$$

Geometric phase:

$$\gamma_n = \int_{\lambda_0}^{\lambda_t} d\lambda \langle \psi_n | i \frac{\partial}{\partial \lambda} | \psi_n \rangle$$



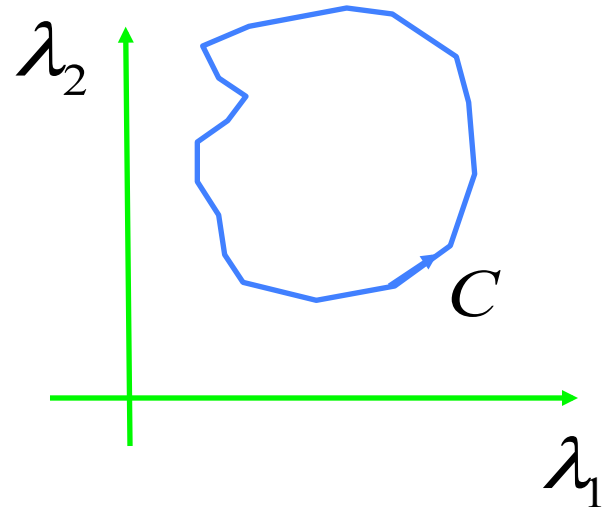


Well defined for a closed path

$$\gamma_n = \oint_C d\lambda \langle \psi_n | i \frac{\partial}{\partial \lambda} | \psi_n \rangle$$

Stokes theorem

$$\gamma_n = \iint d\lambda_1 d\lambda_2 \Omega$$



Berry Curvature

$$\Omega = i \frac{\partial}{\partial \lambda_1} \langle \psi | \frac{\partial}{\partial \lambda_2} | \psi \rangle - i \frac{\partial}{\partial \lambda_2} \langle \psi | \frac{\partial}{\partial \lambda_1} | \psi \rangle$$

# Analogies

Berry curvature

$$\Omega(\vec{\lambda})$$

Berry connection

$$\langle \psi | i \frac{\partial}{\partial \lambda} | \psi \rangle$$

Geometric phase

$$\oint d\lambda \langle \psi | i \frac{\partial}{\partial \lambda} | \psi \rangle = \iint d^2 \lambda \Omega(\vec{\lambda})$$

Chern number

$$\iint d^2 \lambda \Omega(\vec{\lambda}) = \text{integer}$$

Magnetic field

$$B(\vec{r})$$

Vector potential

$$A(\vec{r})$$

Aharonov-Bohm phase

$$\oint dr A(\vec{r}) = \iint d^2 r B(\vec{r})$$

Dirac monopole

$$\iint d^2 r B(\vec{r}) = \text{integer } h/e$$

## (2) Semiclassical dynamics of Bloch electrons

Old version [e.g., Ashcroft, Mermin, 1976]

$$\dot{\mathbf{x}}_c = \frac{1}{\hbar} \frac{\partial \varepsilon_n(\mathbf{k})}{\partial \mathbf{k}},$$

$$\dot{\mathbf{k}} = -\frac{e}{\hbar} \mathbf{E} - \frac{e}{\hbar} \dot{\mathbf{x}}_c \times \mathbf{B} = \frac{e}{\hbar} \frac{\partial \varphi(\mathbf{r})}{\partial \mathbf{r}} - \frac{e}{\hbar} \dot{\mathbf{x}}_c \times \mathbf{B}.$$

Berry phase correction [Chang & Niu, PRL (1995), PRB (1996)]

New version [Marder, 2000]

$$\dot{\mathbf{x}}_c = \frac{1}{\hbar} \frac{\partial \varepsilon_n(\mathbf{k})}{\partial \mathbf{k}} - \dot{\mathbf{k}} \times \mathbf{\Omega}_n(\mathbf{k}),$$

$$\dot{\mathbf{k}} = \frac{e}{\hbar} \frac{\partial \varphi(\mathbf{r})}{\partial \mathbf{r}} - \frac{e}{\hbar} \dot{\mathbf{x}}_c \times \mathbf{B},$$

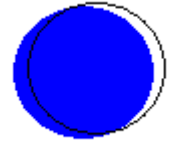
$$\mathbf{\Omega}_n(\mathbf{k}) = -\text{Im} \left\langle \frac{\partial u_{n\mathbf{k}}}{\partial \mathbf{k}} \left| \times \right| \frac{\partial u_{n\mathbf{k}}}{\partial \mathbf{k}} \right\rangle. \quad (\text{Berry curvature})$$

### (3) Semiclassical transport theory

$$\mathbf{j} = \int d^3k (-e\mathbf{v}) g(\mathbf{r}, \mathbf{k}), \quad g(\mathbf{r}, \mathbf{k}) = f(\mathbf{k}) + \delta f(\mathbf{r}, \mathbf{k})$$

$$\mathbf{v} = \frac{\partial \varepsilon_n(\mathbf{k})}{\hbar \partial \mathbf{k}} + \frac{e}{\hbar} \mathbf{E} \times \boldsymbol{\Omega}$$

(ordinary conductance)



$$\mathbf{j} = -\frac{e^2}{\hbar} \mathbf{E} \times \int d^3k f(\mathbf{k}) \boldsymbol{\Omega} - \frac{e}{\hbar} \int d^3k \delta f(\mathbf{k}, \mathbf{r}) \frac{\partial \varepsilon_n(\mathbf{k})}{\partial \mathbf{k}}$$

(Anomalous Hall conductance)

### Anomalous Hall conductivity

$$\sigma_{xy} = -\frac{e^2}{\hbar} \int d^3k \sum_n f(\varepsilon_n(\mathbf{k})) \Omega_n^z(\mathbf{k})$$

$$\Omega_n^z(\mathbf{k}) = -\sum_{n' \neq n} \frac{2 \operatorname{Im} \langle \mathbf{k}n | v_x | \mathbf{k}n' \rangle \langle \mathbf{k}n' | v_y | \mathbf{k}n \rangle}{(\omega_{\mathbf{k}n'} - \omega_{\mathbf{k}n})^2}$$

[FLAPW (WIEN2k) calculations]

$\sigma_{xy}$ (S/cm)	theory	Exp.
bcc Fe	750 <sup>a</sup>	1030
hcp Co	477 <sup>b</sup>	480
fcc Ni	-1066 <sup>c</sup>	-1100

<sup>a</sup>[Yao, et al., PRL 92 (2004) 037204]

<sup>b</sup>[Wang, et al., PRB 76 (2007) 195109]

<sup>c</sup>[Fuh, Guo, PRB 84 (2011) 144427]

## (4) *Ab initio* relativistic band structure methods

Calculations must be based on a relativistic band theory because all the intrinsic Hall effects are caused by spin-orbit coupling.

Relativistic extension of linear muffin-tin orbital (LMTO) method.

[Ebert, PRB 1988; Guo & Ebert, PRB 51, 12633 (1995)]

$$\text{Dirac Hamiltonian} \quad H_D = c\boldsymbol{\alpha} \cdot \mathbf{p} + mc^2(\beta - I) + v(\mathbf{r})I$$

$$\sigma_{xy} = \frac{e}{\hbar} \int d^3\mathbf{k} \sum_n f(\varepsilon_n(\mathbf{k})) \Omega_n^z(\mathbf{k})$$

$$\Omega_n^z(\mathbf{k}) = - \sum_{n' \neq n} \frac{2 \operatorname{Im} \langle \mathbf{k}n | j_x | \mathbf{k}n' \rangle \langle \mathbf{k}n' | v_y | \mathbf{k}n \rangle}{(\omega_{\mathbf{k}n} - \omega_{\mathbf{k}n'})^2}$$

$$\text{current operator } \mathbf{j} = -e c \boldsymbol{\alpha} \quad (\text{AHE}), \quad (\text{charge current operator})$$

$$\mathbf{j} = \frac{\hbar}{4} \{ \beta \Sigma_z, c \boldsymbol{\alpha}_i \} \quad (\text{SHE}), \quad (\text{spin current operator})$$

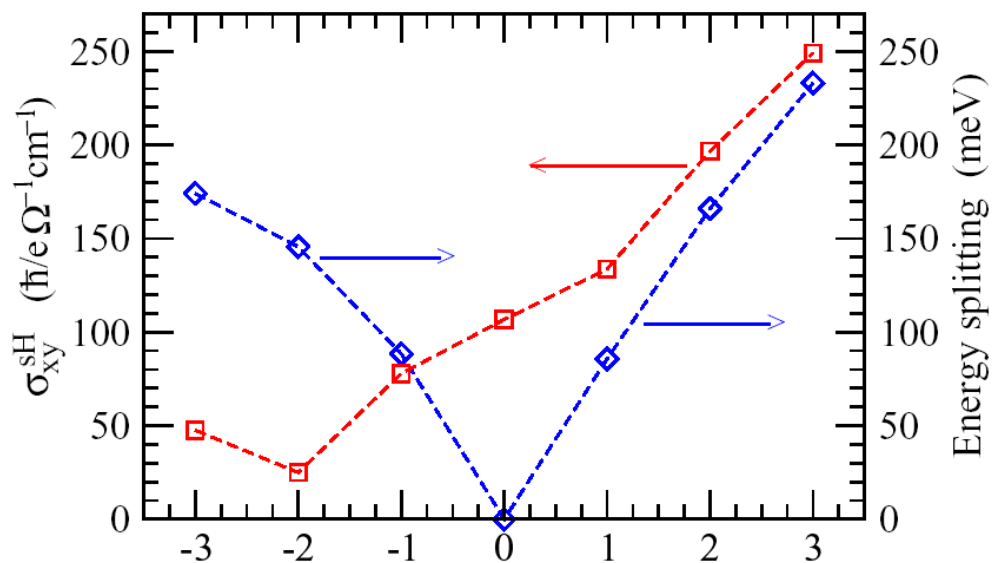
$$\mathbf{j} = \frac{\hbar}{2} \{ \beta L_z, c \boldsymbol{\alpha} \} \quad (\text{OHE}). \quad (\text{orbital current operator})$$

$\boldsymbol{\alpha}$ ,  $\beta$ ,  $\Sigma$  are  $4 \times 4$  Dirac matrices.

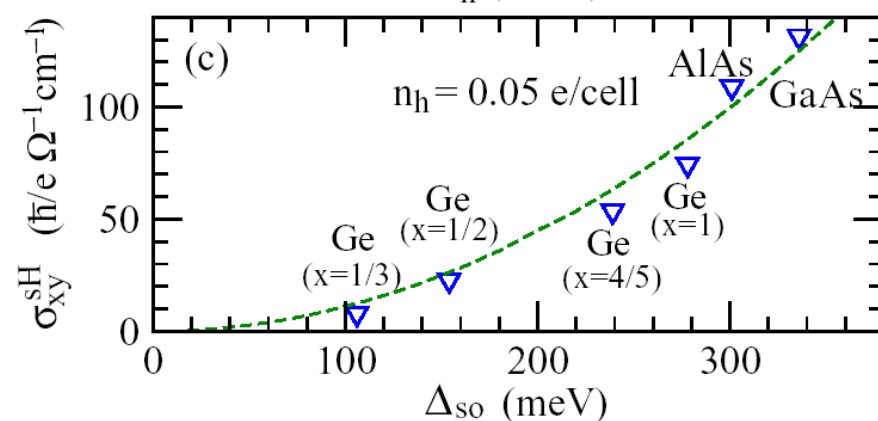
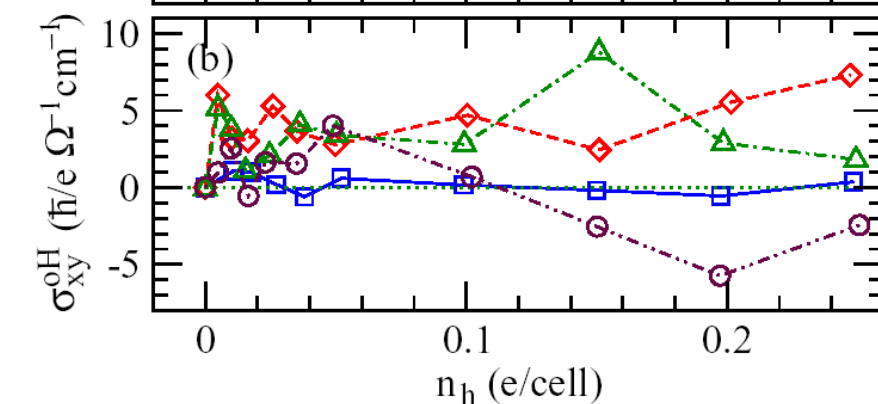
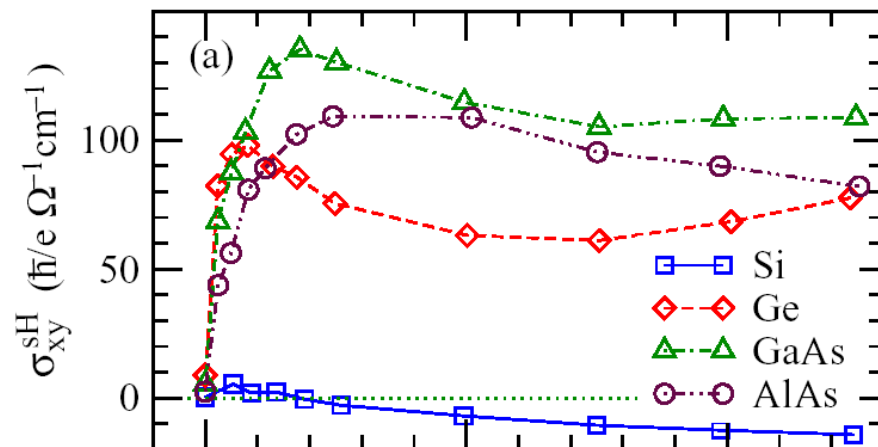
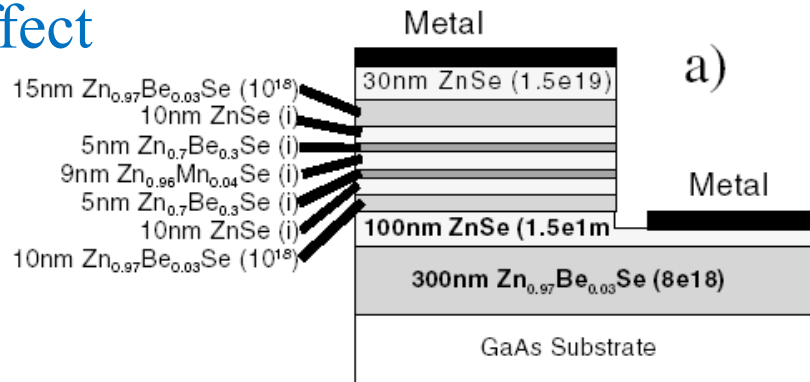
# (5) Application to intrinsic spin Hall effect in semiconductors

[Guo, Yao, Niu, PRL 94, 226601 (2005)]

Spin and orbital angular momentum Hall effects in p-type zincblende semiconductors



Strain effect



## 2. Large intrinsic spin Hall effect in platinum

### Direct electronic measurement of the spin Hall effect

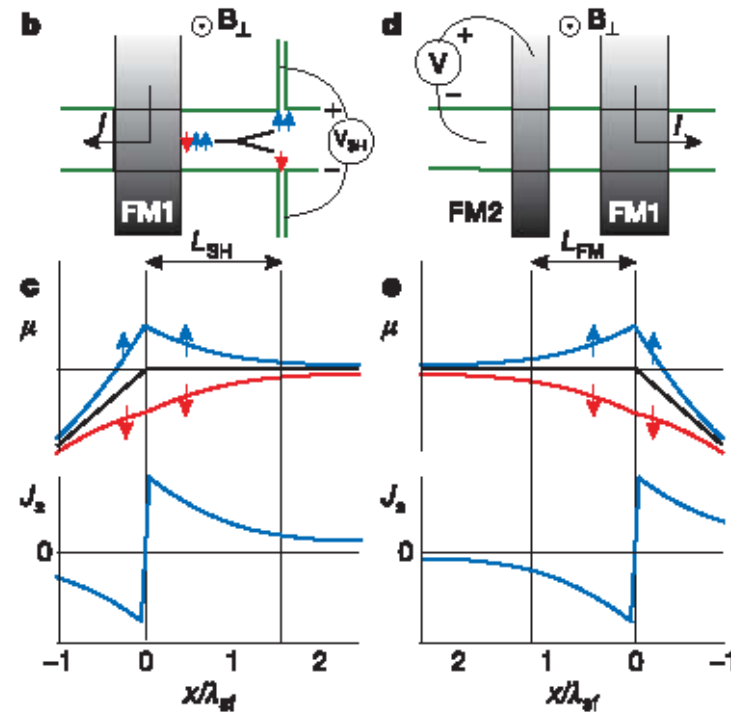
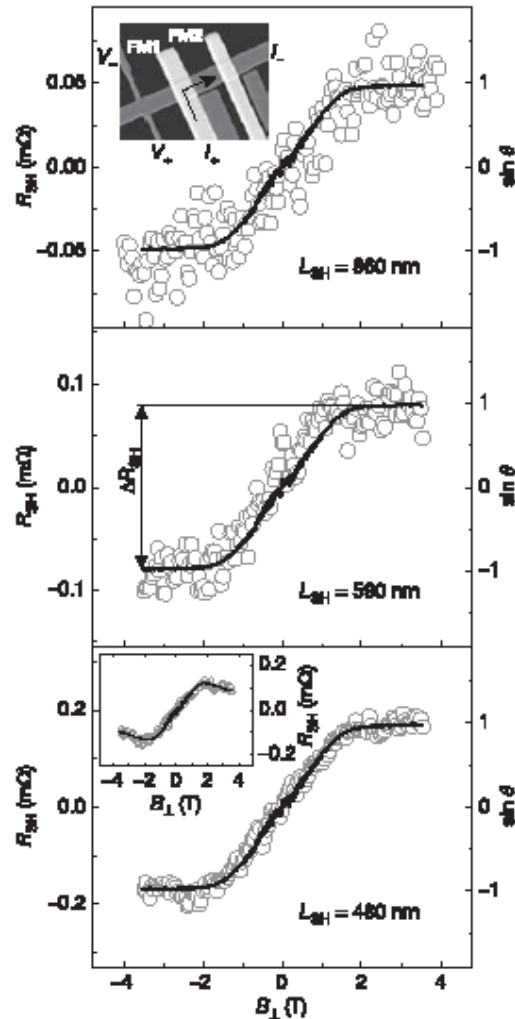
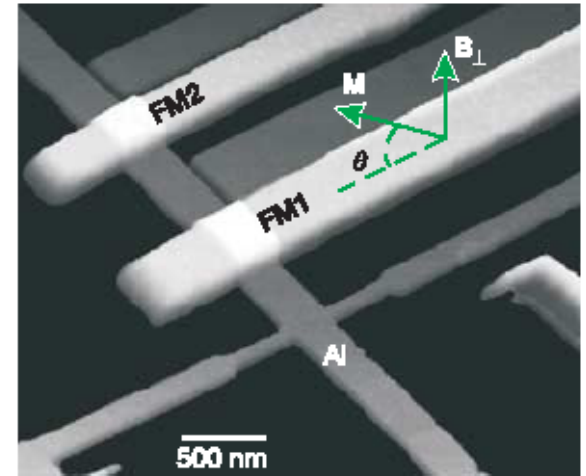
S. O. Valenzuela<sup>1</sup>† & M. Tinkham<sup>1</sup>

Nature 13 July 2006 Vol. 442.

fcc Al

$$\sigma_{\text{SH}} = 27\sim 34 (\Omega\text{cm})^{-1}$$

( $T = 4.2 \text{ K}$ )

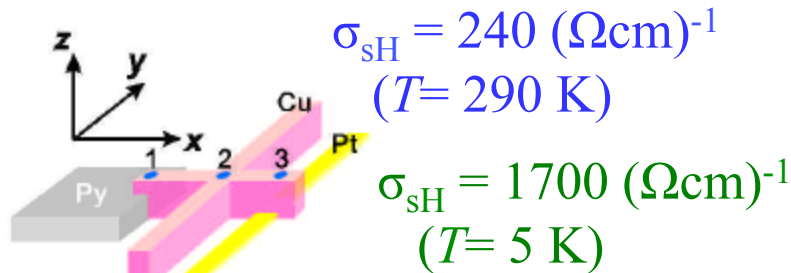
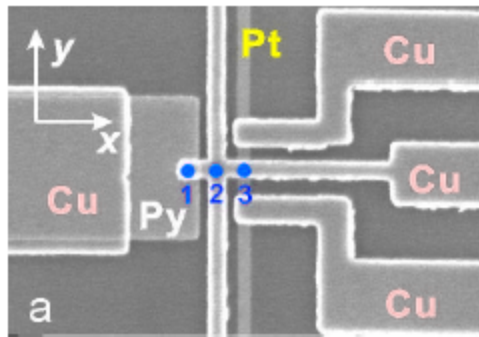


# Room Temperature Reversible Spin Hall Effect

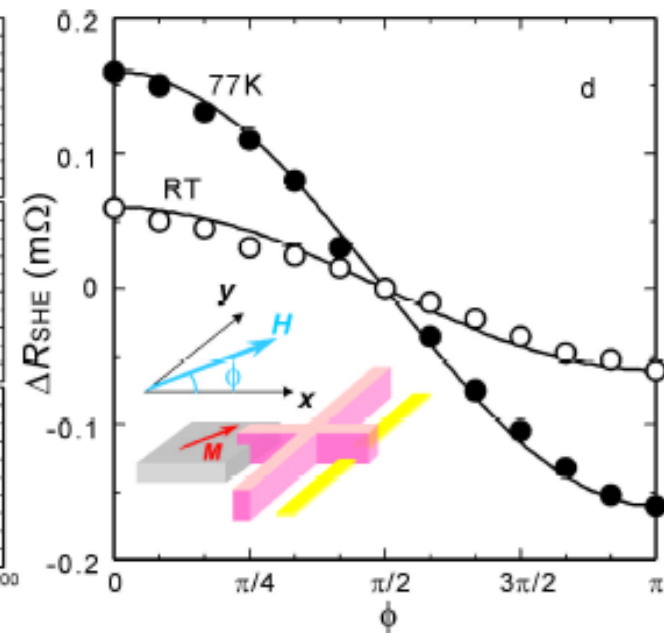
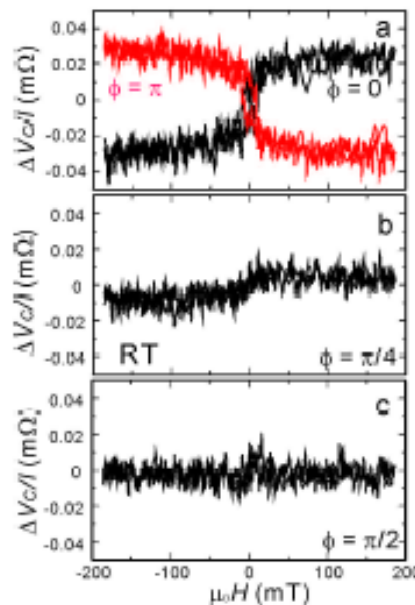
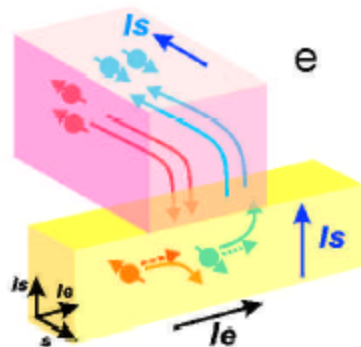
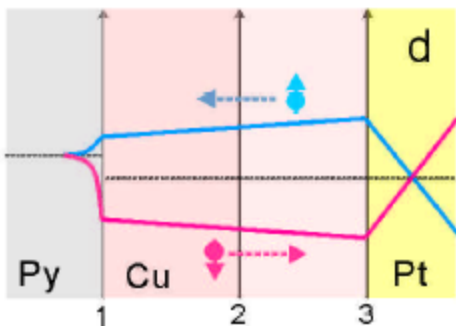
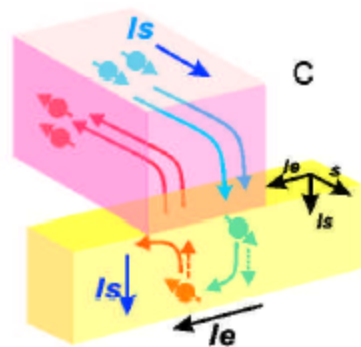
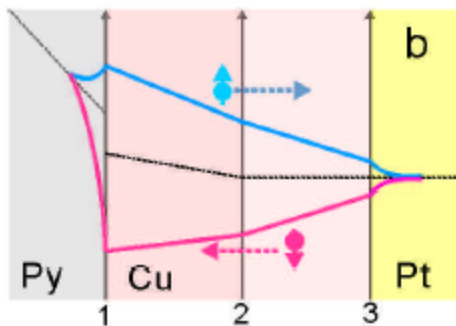
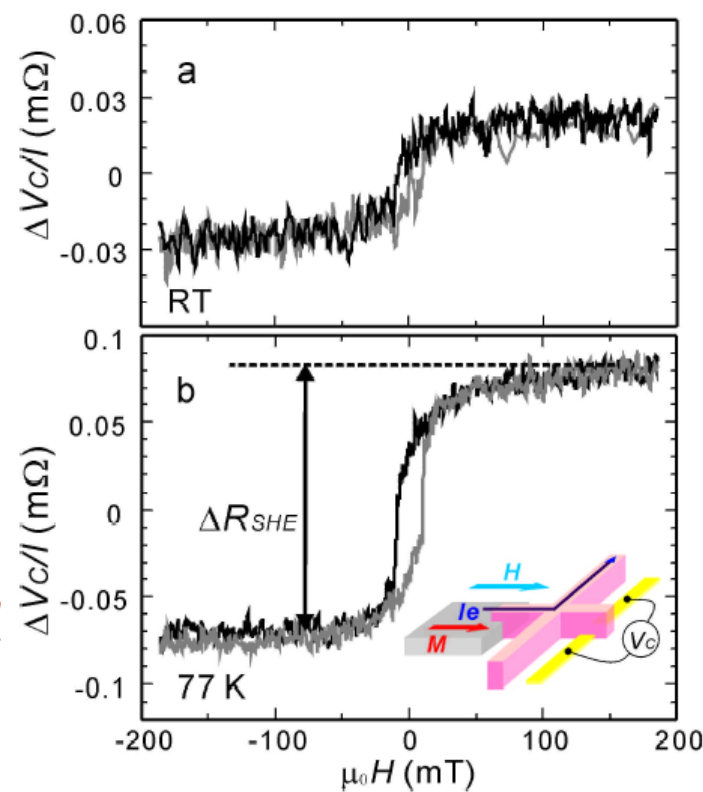
[PRL98 (2007) 156601; PRB83 (2011) 174405 (2011)]

T. Kimura,<sup>1,2</sup> Y. Otani,<sup>1,2</sup> T. Sato,<sup>1</sup> S. Takahashi,<sup>3,4</sup> and S. Maekawa<sup>3,4</sup>

<sup>1</sup> Institute for Solid State Physics, University of Tokyo



Assumed to be extrinsic!

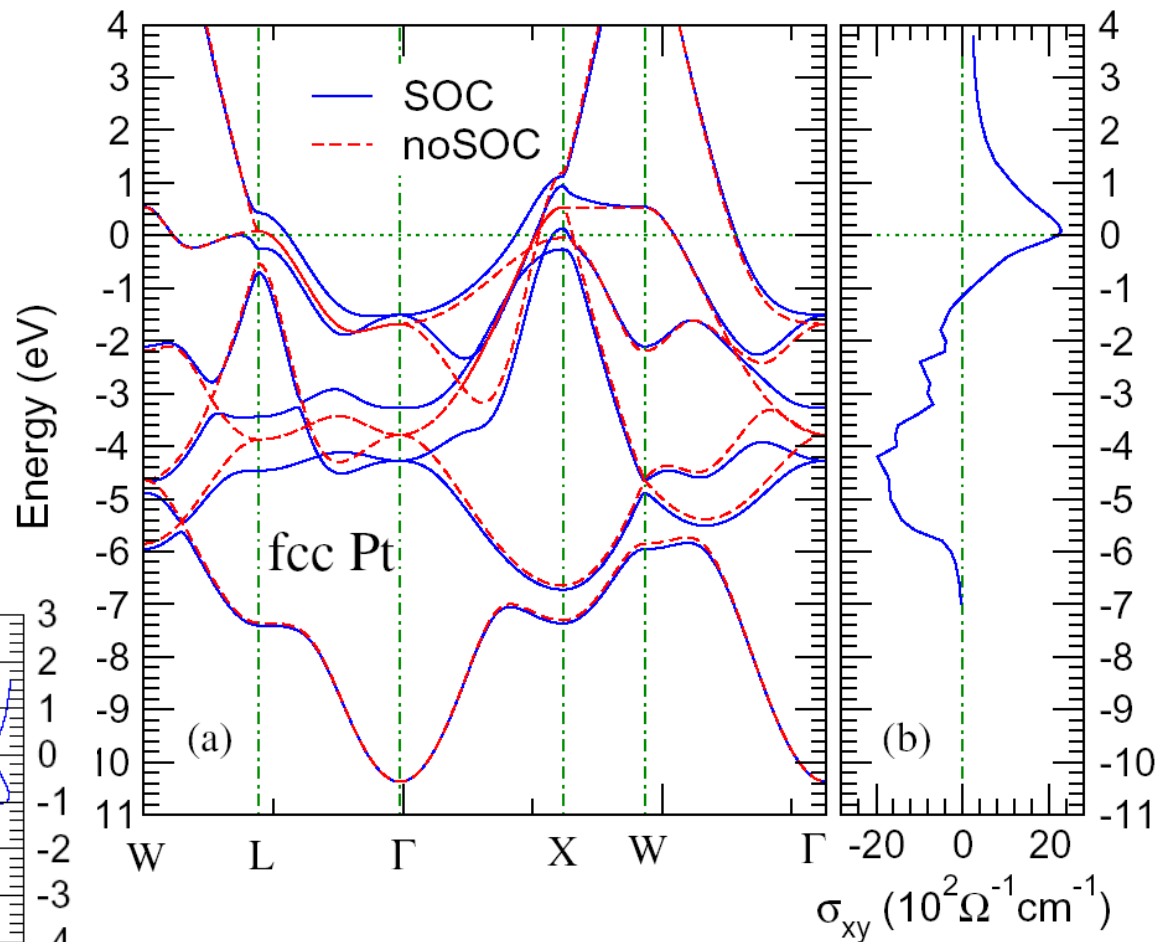
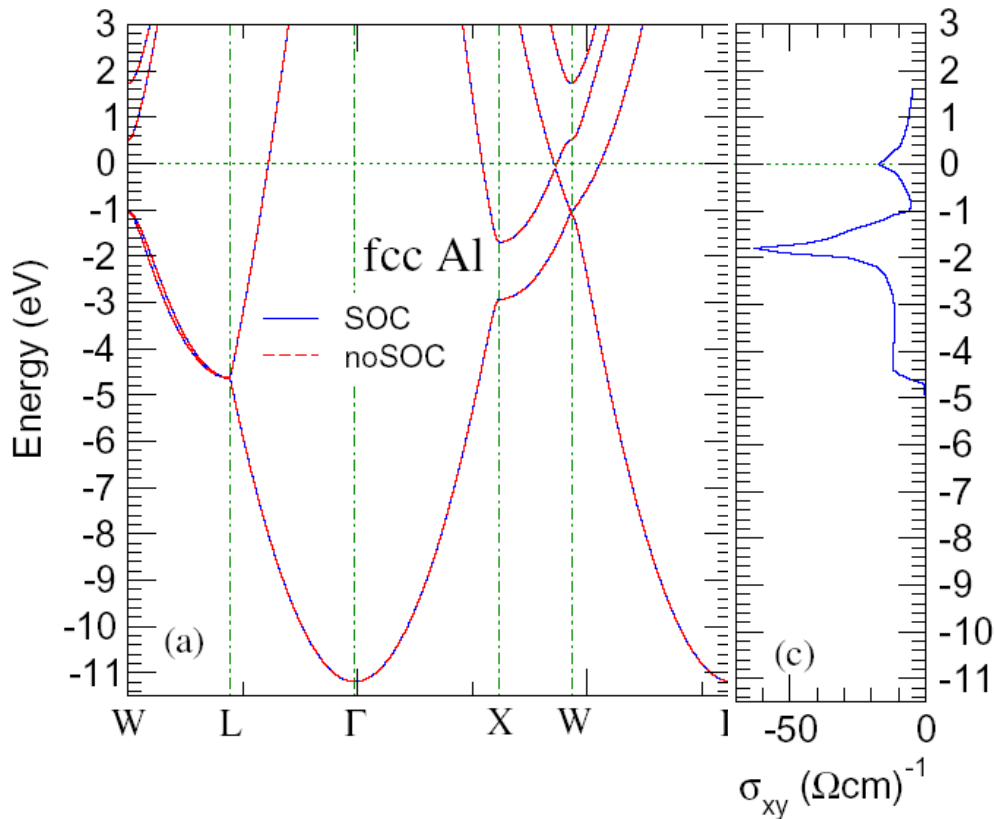




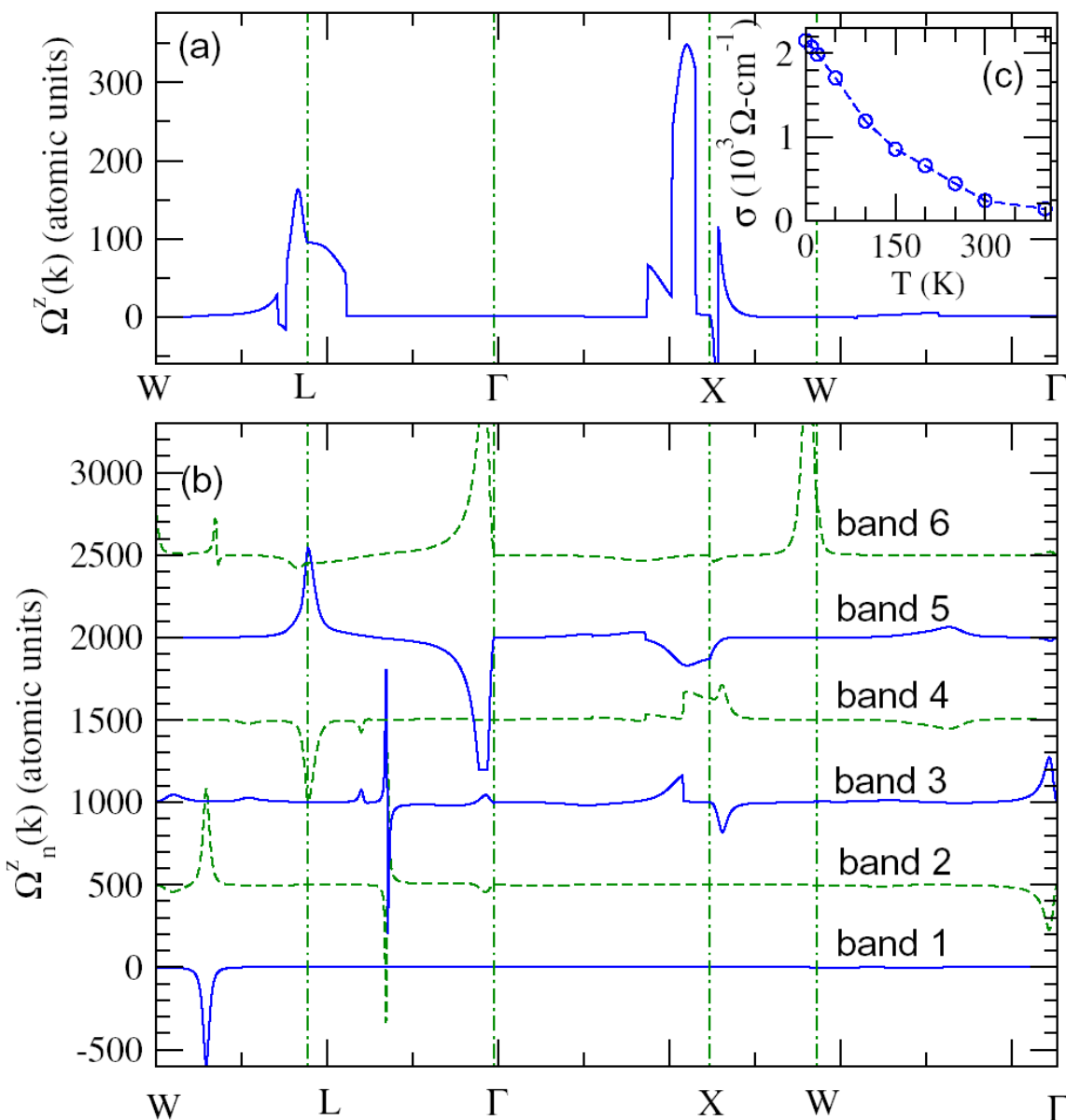
# *Ab initio* relativistic band structure calculations

Pt:  $\sigma_{\text{sH}} = 2200 \text{ (}\Omega\text{cm)}^{-1}$   
( $T = 0 \text{ K}$ )

Al:  $\sigma_{\text{sH}} = 17 \text{ (}\Omega\text{cm)}^{-1}$   
( $T = 0 \text{ K}$ )



[Guo, Murakami, Chen, Nagaosa,  
PRL100, 096401 (2008)]



$$\sigma_{xy} = -\frac{e}{h} \sum_{\mathbf{k}} \Omega^z(\mathbf{k}) = \frac{e}{h} \sum_{\mathbf{k}} \sum_n f(\varepsilon_n(\mathbf{k})) \Omega_n^z(\mathbf{k})$$

$$\Omega_n^z(\mathbf{k}) = \sum_{n' \neq n} \frac{2 \operatorname{Im} \langle \mathbf{k}n | j_x^z | \mathbf{k}n' \rangle \langle \mathbf{k}n' | v_y | \mathbf{k}n \rangle}{(\omega_{\mathbf{k}n} - \omega_{\mathbf{k}n'})^2}$$

Pt:  $\sigma_{\text{sH}}(0\text{K}) = 2200 (\Omega\text{cm})^{-1}$

$\sigma_{\text{sH}}(\text{exp., } 5 \text{ K}) = 1700 (\Omega\text{cm})^{-1}$

[Morota et al, PRB83, 174405 (2011)]

Pt:  $\sigma_{\text{sH}}(300\text{K}) = 240 (\Omega\text{cm})^{-1}$

$\sigma_{\text{sH}}(\text{exp., RT}) = 240 (\Omega\text{cm})^{-1}$

[Kimura et al PRL98, 156601 (2007)]

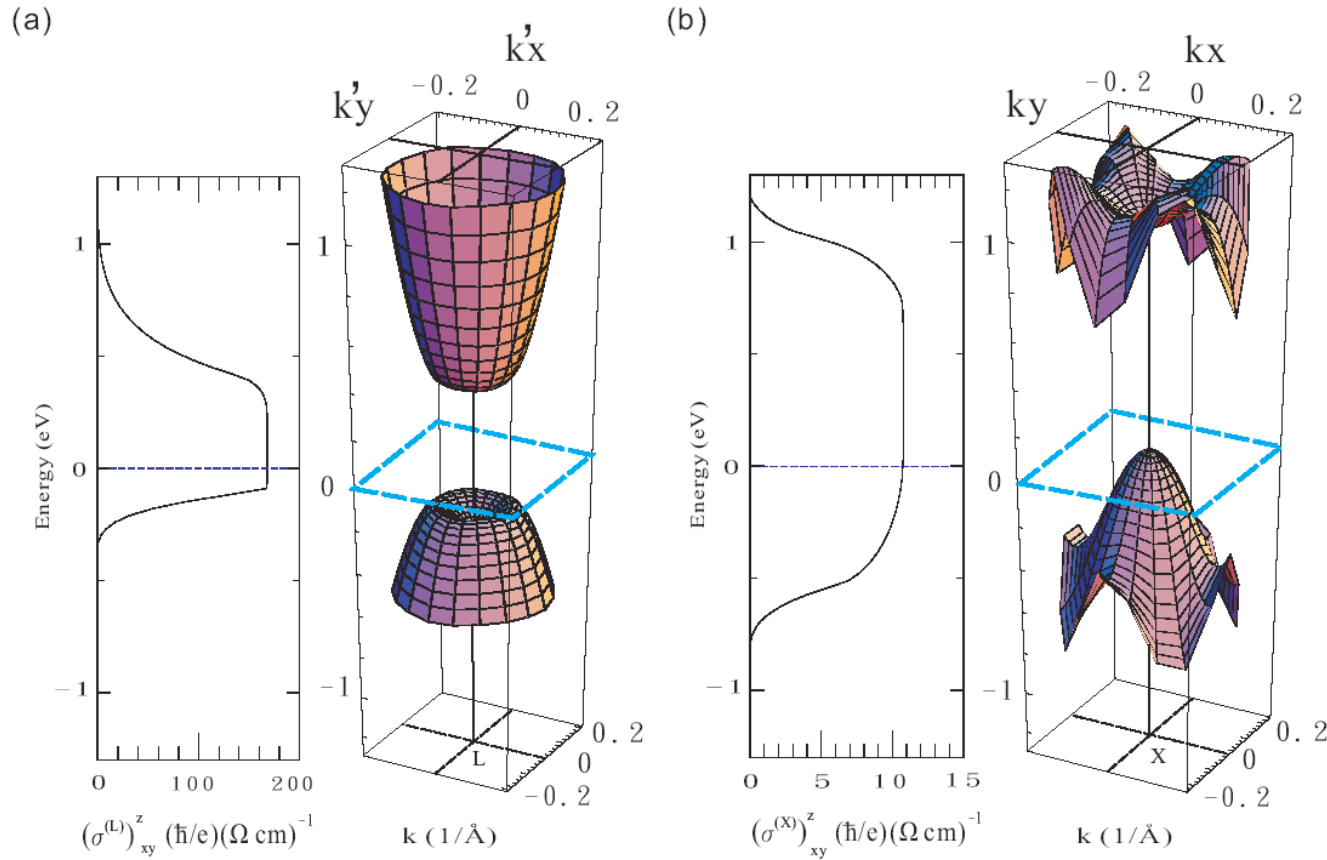
Al:  $\sigma_{\text{sH}}(4.2 \text{ K}) = 17 (\Omega\text{cm})^{-1}$

$\sigma_{\text{sH}}(300 \text{ K}) = 6 (\Omega\text{cm})^{-1}$

$\sigma_{\text{sH}}(\text{exp., } 4.2\text{K}) = 27, 34 (\Omega\text{cm})^{-1}$

[Valenzuela, Tinkham, Nature 442, 176 (2006)]

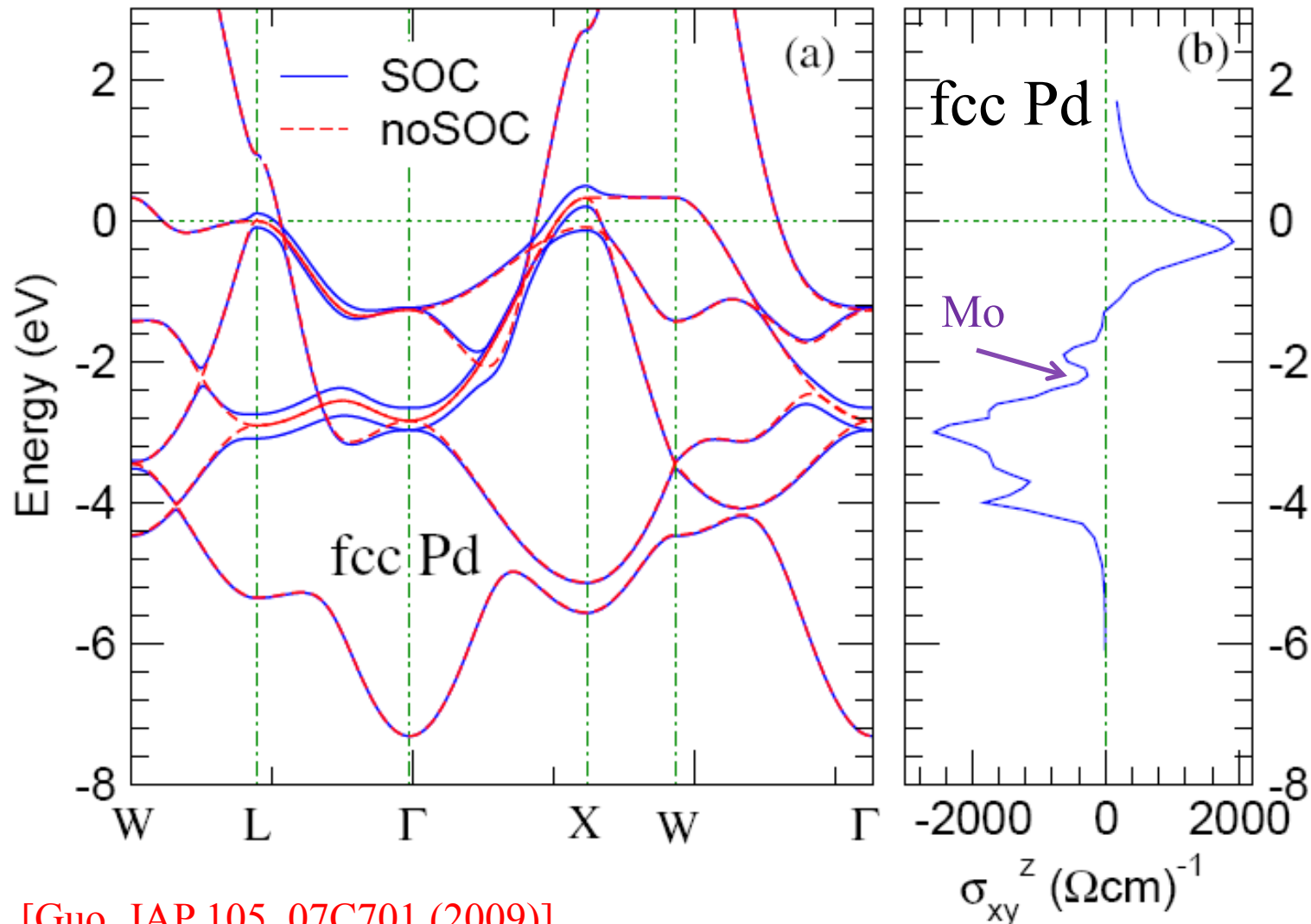
# Effect of impurity scattering and two band model analysis



$$\begin{array}{c}
 \mathbf{j}_x^z \\
 \begin{array}{c}
 \mathbf{k} \quad \mathbf{k}' \\
 \mathbf{k} \quad \mathbf{k}'' \\
 \mathbf{k} \quad \mathbf{k}' \\
 \mathbf{k} \quad \mathbf{k}''
 \end{array} \\
 \mathbf{j}_y
 \end{array}
 +
 \begin{array}{c}
 \mathbf{j}_x^z \\
 \begin{array}{c}
 \mathbf{k} \quad \mathbf{k}' \\
 \mathbf{k} \quad \mathbf{k}'' \\
 \mathbf{k} \quad \mathbf{k}' \\
 \mathbf{k} \quad \mathbf{k}''
 \end{array} \\
 \mathbf{j}_y
 \end{array}
 = 0$$

Intrinsic SHE is robust against short-ranged impurity scattering!

### 3. Intrinsic spin Hall effect in other pure 4d and 5d metals



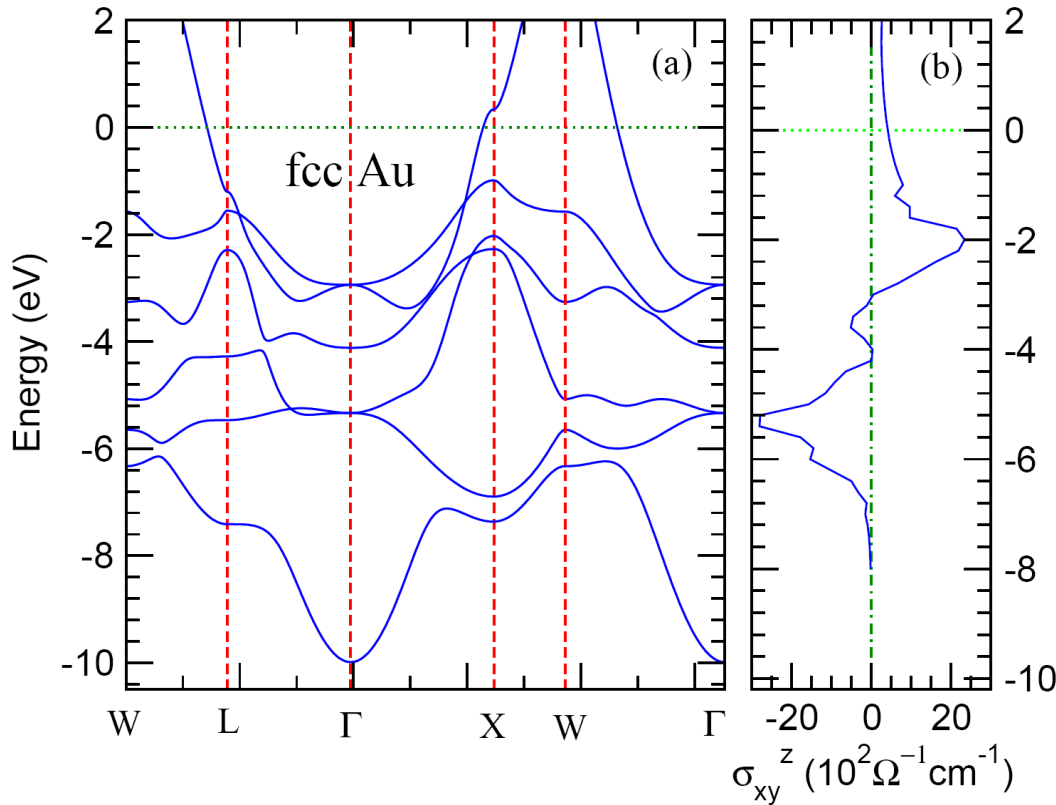
[Guo, JAP 105, 07C701 (2009)]

Pd:  $\sigma_{\text{SH}}(0\text{ K}) = 1400 (\Omega\text{cm})^{-1}$   
 $\sigma_{\text{SH}}(300\text{ K}) = 300 (\Omega\text{cm})^{-1}$

[Morota, et al., JAP 105, 07C712 (2009)]

Mo:  $\sigma_{\text{SH}}(10\text{ K}) = -70 (\Omega\text{cm})^{-1}$   
 $\alpha_{\text{SH}}(10\text{ K}) = -0.002$

# Intrinsic spin Hall effect in pure Au and other metals



<sup>a</sup>[Morota, et al., PRB 83 (2011) 174405]

$$\text{Au: } \sigma_{\text{SH}} = 415 (\Omega\text{cm})^{-1} (T = 0 \text{ K})$$

$$= 750 (\Omega\text{cm})^{-1} (T = 300 \text{ K})$$

[Guo, JAP 105, 07C701 (2009)]

$$\sigma_{\text{SH}} (\text{exp., RT}) = 882 (\Omega\text{cm})^{-1}$$

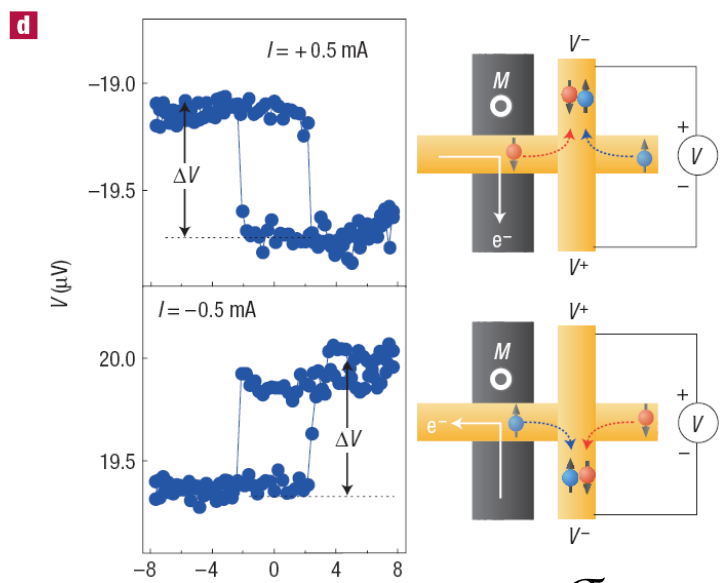
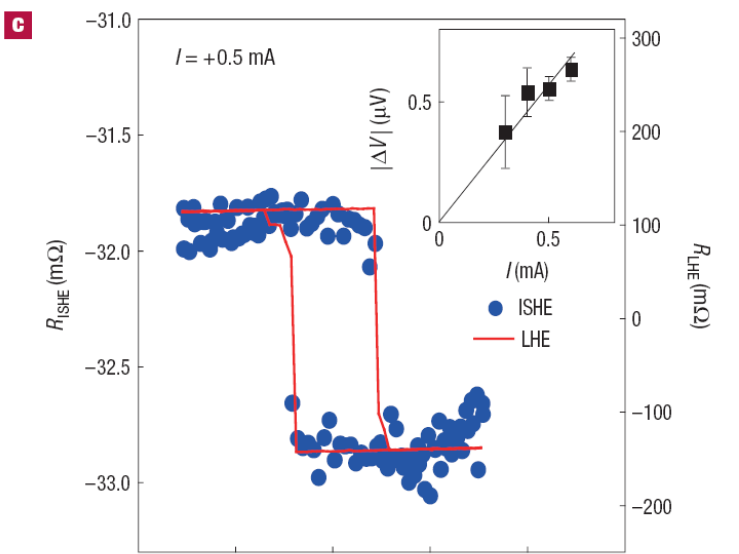
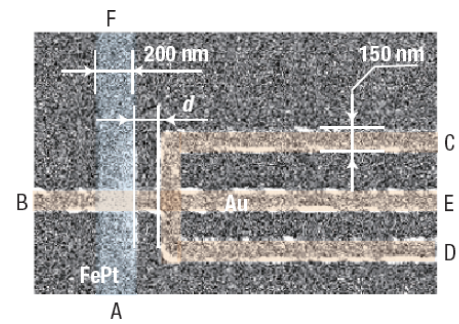
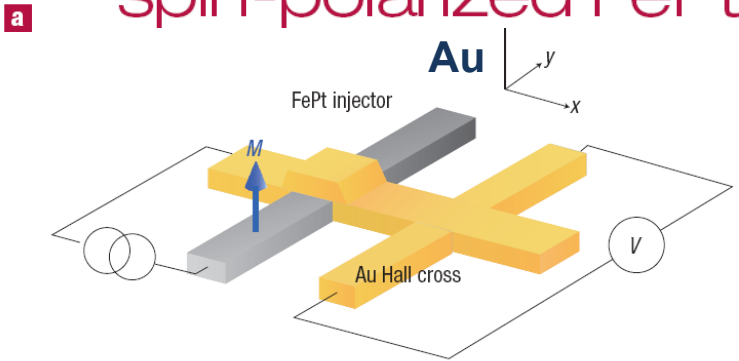
<sup>b</sup>[Mosendz, et al., PRB 82 (2010) 214403]

	$\sigma_{xy}^z$ (0 K) [ $\frac{\hbar}{e}$ (S/cm)]	$\sigma_{xy}^z$ (300 K) [ $\frac{\hbar}{e}$ (S/cm)]
bcc Nb	-164 (-100 <sup>a</sup> )	-167
bcc Mo	-323 (-230 <sup>a</sup> )	-407 (-23 <sup>b</sup> )
bcc Ta	-211 (-11 <sup>a</sup> )	-156
bcc W	-1009	-1037
fcc Pd	1400 <sup>c</sup> (270 <sup>a</sup> )	350 (256 <sup>b</sup> )
fcc Pt	2200 (1700 <sup>a</sup> )	240 (312 <sup>b</sup> )
fcc Au	415 <sup>d</sup>	750 (882 <sup>b</sup> )

# III. Giant spin Hall effect in gold and multi-orbital Kondo effect

## 1. Giant spin Hall effect in perpendicularly spin-polarized FePt/Au devices

[Seki, et al., Nat. Mater. 7 (2008)125]



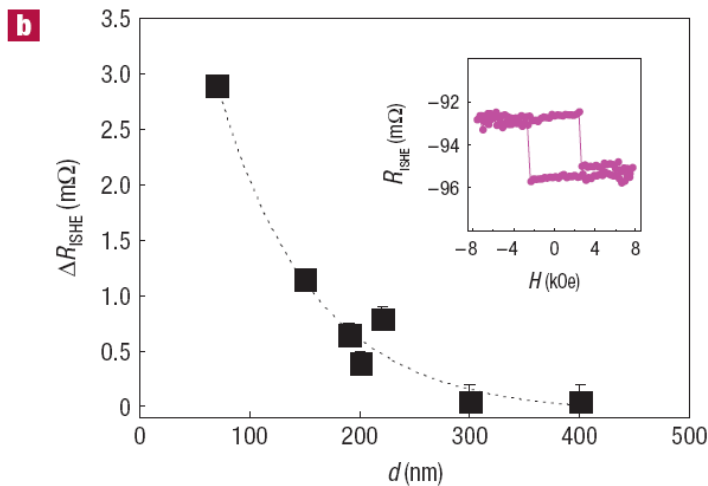
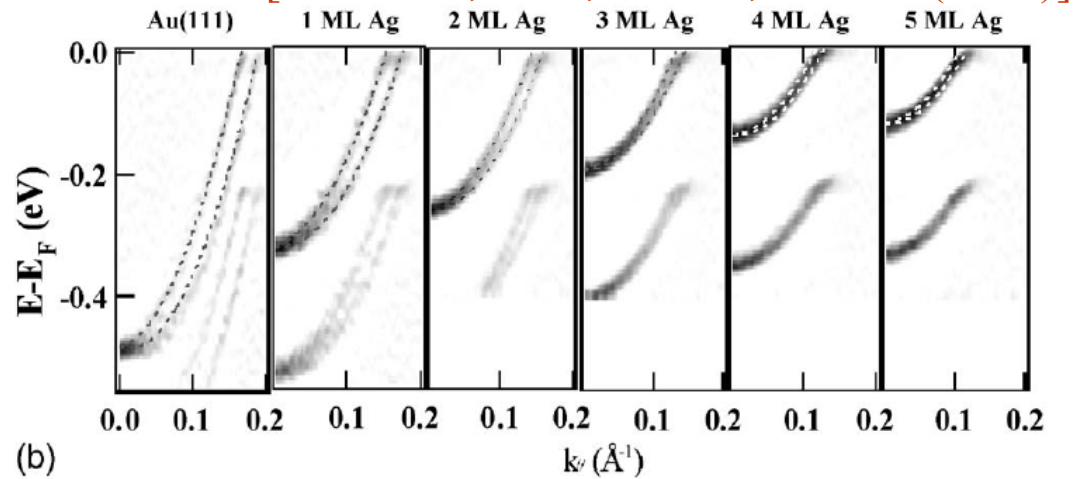
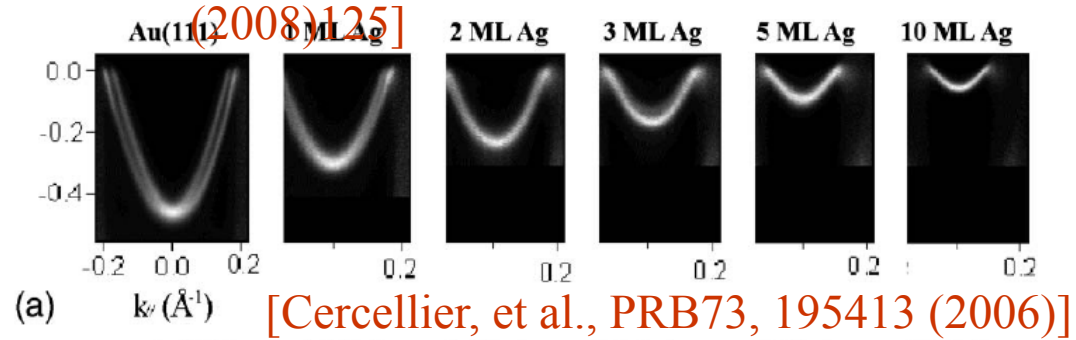
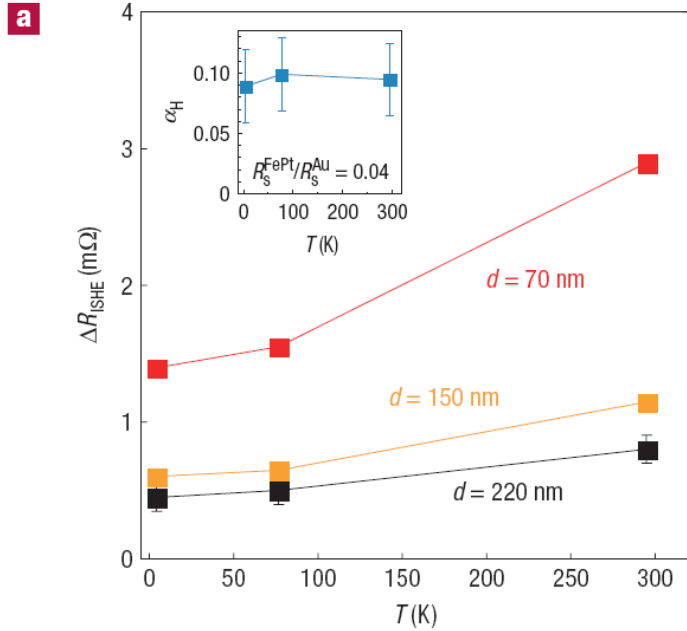
$$\sigma_{SHE} \approx 10^5 \Omega^{-1} \text{cm}^{-1}$$

$$\Delta R_{ISHE} = 2\alpha_H \frac{\rho_{Au}}{t_{Au}} P \exp(-d/\lambda_{Au}),$$

spin Hall angle  $\alpha_H = \frac{\sigma_{xy}}{\sigma_{xx}} \approx 0.1$  at RT

# What is the origin of giant spin Hall effect in gold Hall bars?

(i) Surface and interface effect? [Seki, et al., Nat. Mater. 7 (2008)125]



(ii) Defect and impurity origin ?

- Possible impurities: (a) vacancy of Au atom  
 (b) Pt impurity  
 (c) Fe impurity

## 2. Multiorbital Kondo effect in Fe impurity in gold.

### Results of FLAPW calculations

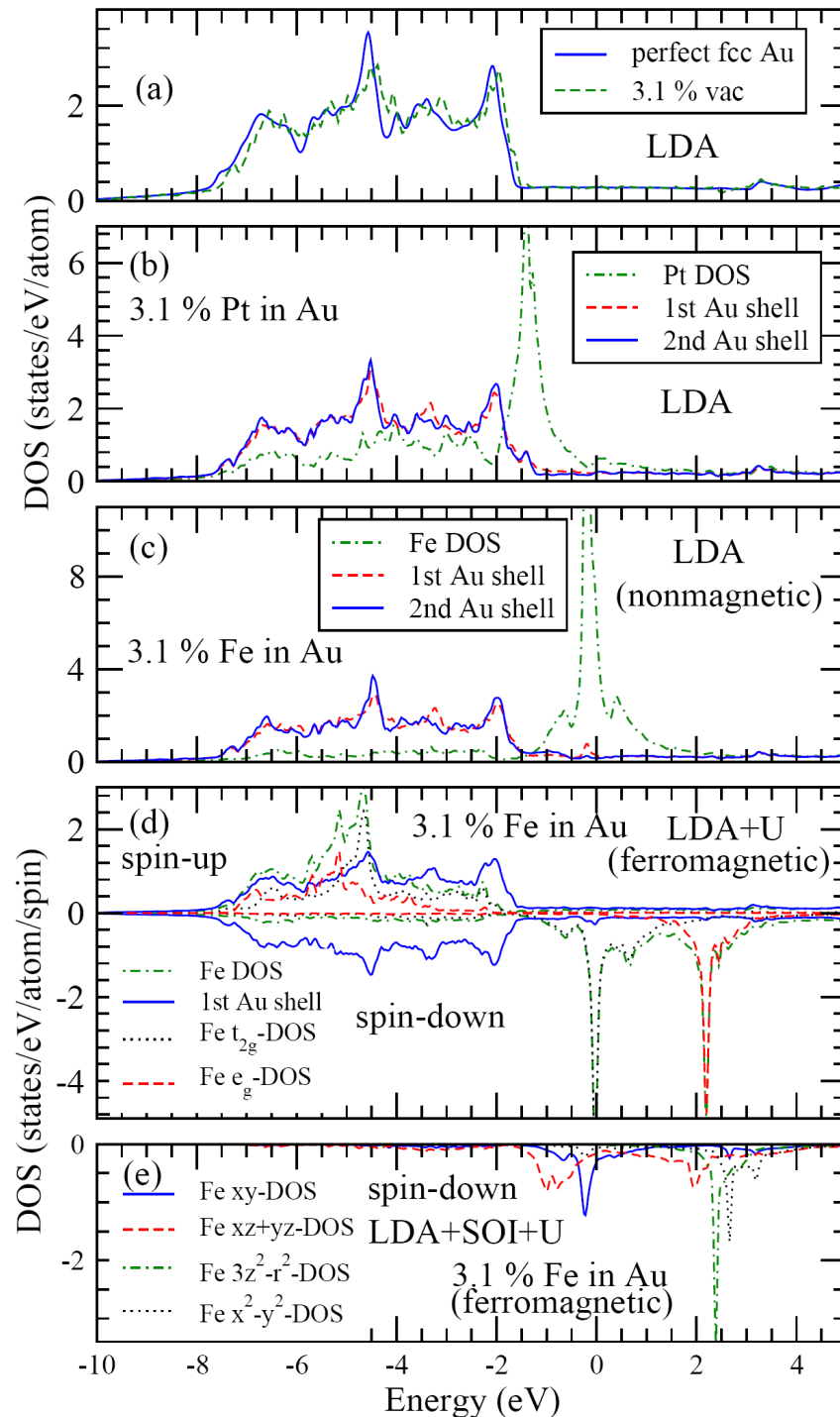
(a) the change in DOS in the 5d bands.

(b) the DOS change is near -1.5 eV.

Nonmagnetic in (a) and (b)

(c) A peak in DOS at the Fermi level and magnetic.

Proposal: Multiorbital Kondo effect in Fe impurity in gold.





### 3. Enhanced SHE by resonant skew scattering in orbital-dependent Kondo effect.

[Guo, Maekawa, Nagaosa, PRL 102, 036401 (2009)]

Extrinsic spin Hall effect due to skew scattering

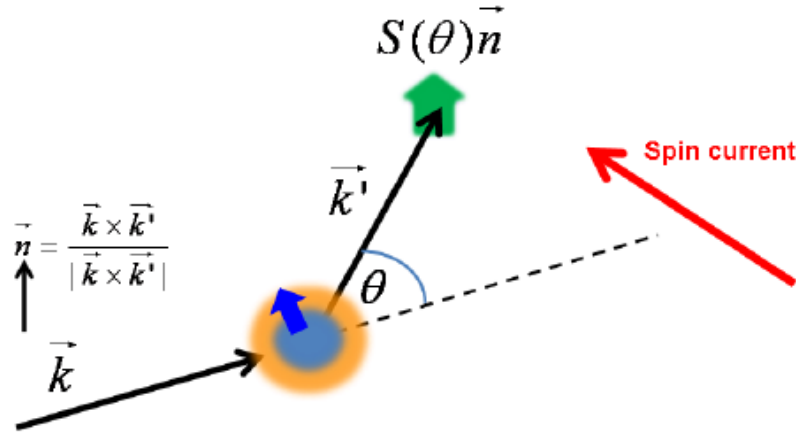


FIG. 1: (color online) The skew scattering due to the spin-orbit interaction of the scatterer and the spin unpolarized electron beam with wavevector  $\vec{k}$  with the angle  $\theta$  with the spin polarization  $S(\theta)\vec{n}$  with  $\vec{n} = (\vec{k} \times \vec{k}')/|\vec{k} \times \vec{k}'|$ .

scattering amplitudes

$$f_{\uparrow}(\theta) = f_1(\theta)|\uparrow\rangle + ie^{i\varphi}f_2(\theta)|\downarrow\rangle$$

$$f_{\downarrow}(\theta) = f_1(\theta)|\downarrow\rangle - ie^{-i\varphi}f_2(\theta)|\uparrow\rangle$$

skewness function

$$S(\theta) = \frac{2\text{Im}[f_1^*(\theta)f_2(\theta)]}{|f_1(\theta)|^2 + |f_2(\theta)|^2}$$

spin Hall angle

$$\gamma_S = \frac{\int d\Omega I(\theta)S(\theta)\sin\theta}{\int d\Omega I(\theta)(1 - \cos\theta)}$$

$$f_1(\theta) = \sum_l \frac{P_l(\cos\theta)}{2ik} \left[ (l+1) \left( e^{2i\delta_l^+} - 1 \right) + l \left( e^{-2i\delta_l^-} - 1 \right) \right]$$

$$f_2(\theta) = \sum_l \frac{\sin\theta}{2ik} \left( e^{2i\delta_l^+} - e^{2i\delta_l^-} \right) \frac{d}{d\cos\theta} P_l(\cos\theta).$$

TABLE I: Down-spin occupation numbers of the 3d-suborbitals of the Fe impurity in Au from LDA+ $U$  calculations without SOI and with SOI. The calculated magnetic moments are:  $m_s^{Fe} = 3.39 \mu_B$  and  $m_s^{tot} = 3.32 \mu_B$  without SOI, as well as  $m_s^{Fe} = 3.19 \mu_B$ ,  $m_o^{Fe} = 1.54 \mu_B$  and  $m_s^{tot} = 3.27 \mu_B$  with SOI. The muffin-tin sphere radius  $R_{mt} = 2.65a_0$  ( $a_0$  is Bohr radius) is used for both Fe and Au atoms.

[Guo, Maekawa, Nagaosa, PRL 102, 036401 (2009)]

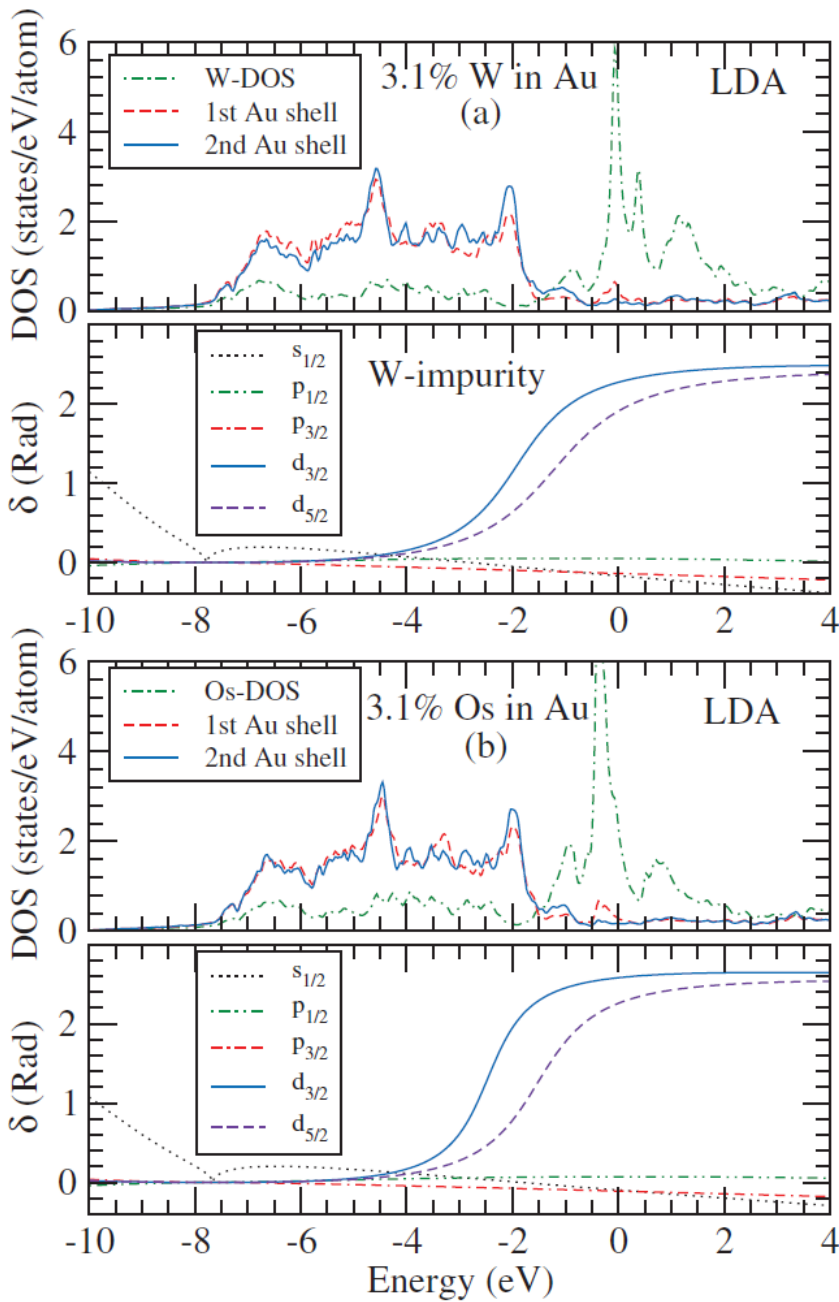
(a)	$xy$	$xz$	$yz$	$3z^2 - r^2$	$x^2 - y^2$
no SOI	0.459	0.459	0.459	0.053	0.053
SOI	0.559	0.453	0.453	0.050	0.128
(b)	$m = -2$	$m = -1$	$m = 0$	$m = 1$	$m = 2$
no SOI	0.256	0.459	0.053	0.459	0.256
SOI	0.138	0.087	0.050	0.819	0.549

Occupation numbers are related to the phase shifts through generalized Friedel sum rule.

$$\gamma_s \cong -\frac{3\delta_1(\cos 2\delta_2^+ - \cos 2\delta_2^-)}{9\sin^2 \delta_2^+ + 4\sin^2 \delta_2^- + 3[1 - \cos 2(\delta_2^+ - \delta_2^-)]}$$

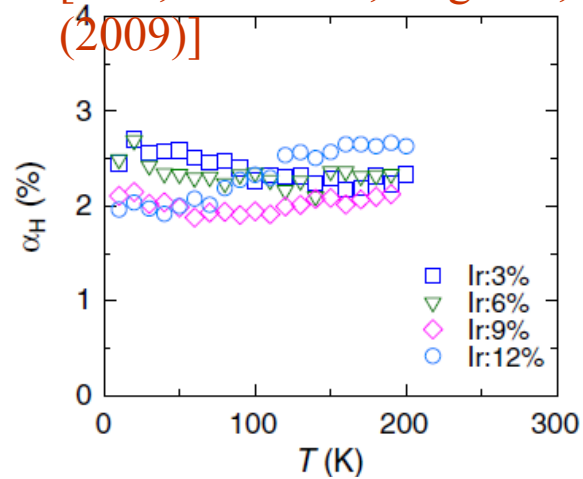
$$\gamma_s \cong \delta_1 \approx 0.1$$

$$\gamma_H \approx 0.001 \sim 0.01 \quad [\text{Fert, et al., JMMM 24 (1981) 231}]$$

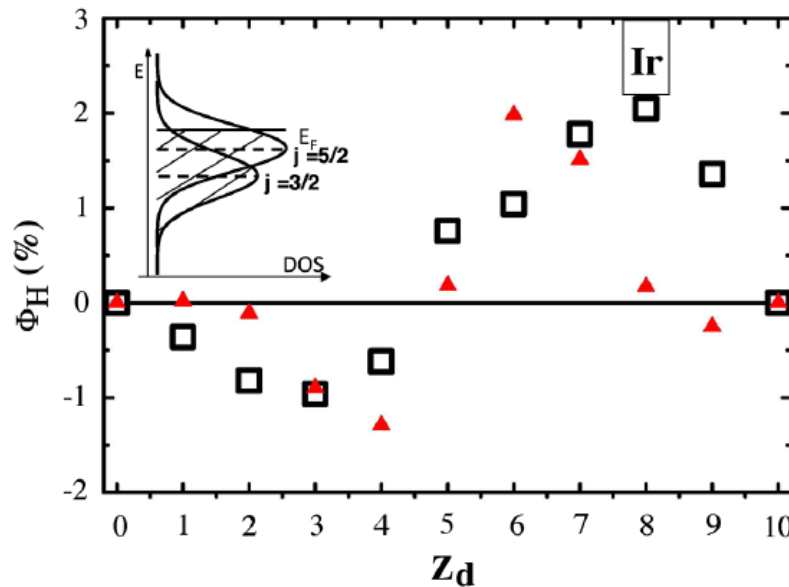


Prediction: Large SHE ( $\gamma_s \sim 4\%$ ) would also occur in 5d impurities in noble metals due to resonant skew scattering.

[Guo, Maekawa, Nagaosa, PRL 102, 036401 (2009)]



[Niimi et al, PRL 106, 126601 (2011)]



[Fert, Levy, PRL 106, 157208 (2011)]

## Viewpoint

## Lending an iron hand to spintronics

Piers Coleman

Department of Physics and Astronomy, Rutgers University, 136 Frelinghuysen Road, Piscataway, NJ 08854-8019, USA

Published January 20, 2009

Subject Areas: Spintronics

A Viewpoint on:

Enhanced Spin Hall Effect by Resonant Skew Scattering in the Orbital-Dependent Kondo Effect

Guang-Yu Guo, Sadamichi Maekawa and Naoto Nagaosa

Phys. Rev. Lett. 102, 036401 (2009) – Published January 20, 2009

Despite its long history, the detailed Kondo physics of iron remains a controversial subject, in part because of the complex orbital structure of the impurity atom. The magnetism of iron in gold is carried by iron's five valence  $d$  electrons, each of which resides in one of five different  $d$  orbitals. On an isolated Fe atom, these  $d$  orbitals are nearly degenerate, but in the cubic environment of the gold crystal, the  $d$  orbitals split up into two components—a doublet, labeled the  $e_g$  orbitals, and a triplet, labeled the  $t_{2g}$  orbitals. During the past year, both Guo *et al.* and a research collaboration of Theo Costi, Achim Rosch, and coworkers [11] have independently proposed that the Kondo effect in iron is "orbitally selective," involving two widely different Kondo temperatures—one for each set of orbitals. Both groups suggest that some of the iron  $d$ -spins delocalize because of the Kondo effect at room temperature, leaving behind two or three remaining electrons that only delocalize around 1 K.

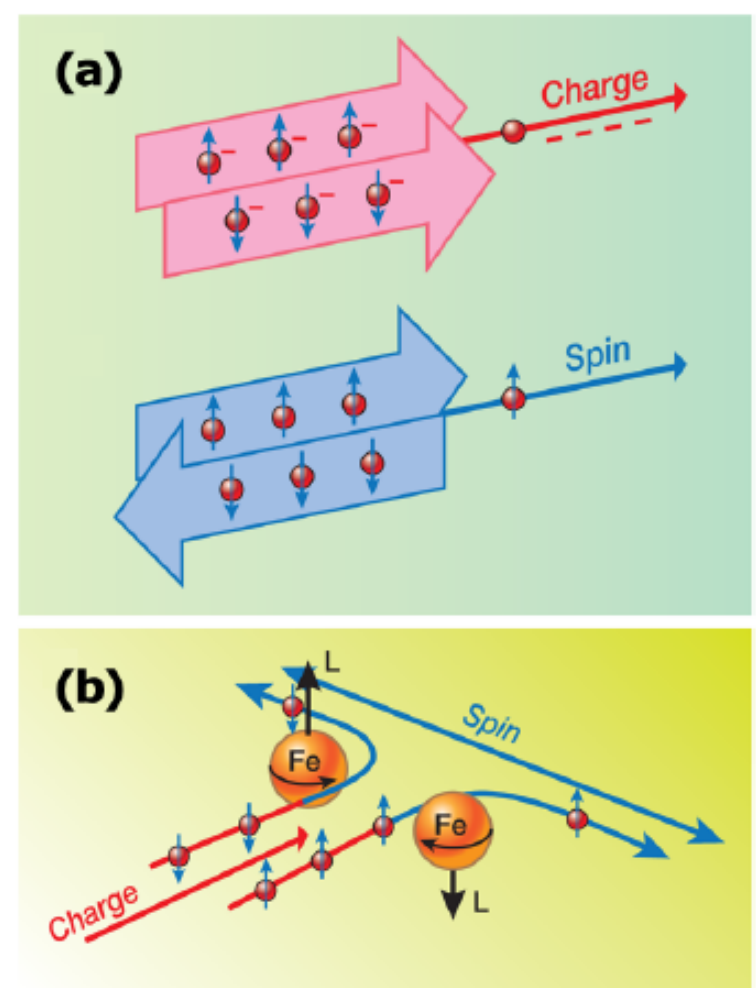


FIG. 1: (a) In a charge current, spin "up" and "down" electrons flow together. In a spin current, up and down electrons flow in opposite directions. (b) A schematic of the spin Hall effect. Spin-orbit coupling induces an orbital motion opposite in direction to the electron spin, deflecting up- and down-spin electrons in opposite directions. The net effect is a conversion of charge into spin currents. (Illustration: Alan Stonebraker/stonebrakerdesignworks.com)

# 4. Quantum Monte Carlo simulation

## 1) problems

## XMCD measurements

VOLUME 93, NUMBER 7

PHYSICAL REVIEW LETTERS

week ending  
13 AUGUST 2004

### Direct Observation of Orbital Magnetism in Cubic Solids

W. D. Brewer,<sup>1,\*</sup> A. Scherz,<sup>1</sup> C. Sorg,<sup>1</sup> H. Wende,<sup>1</sup> K. Baberschke,<sup>1</sup> P. Bencok,<sup>2</sup> and S. Frota-Pessôa<sup>3</sup>

<sup>1</sup>Physikalisches Institut der Universität zu Köln, Zoltanstr. 14, D-50937 Köln, Germany

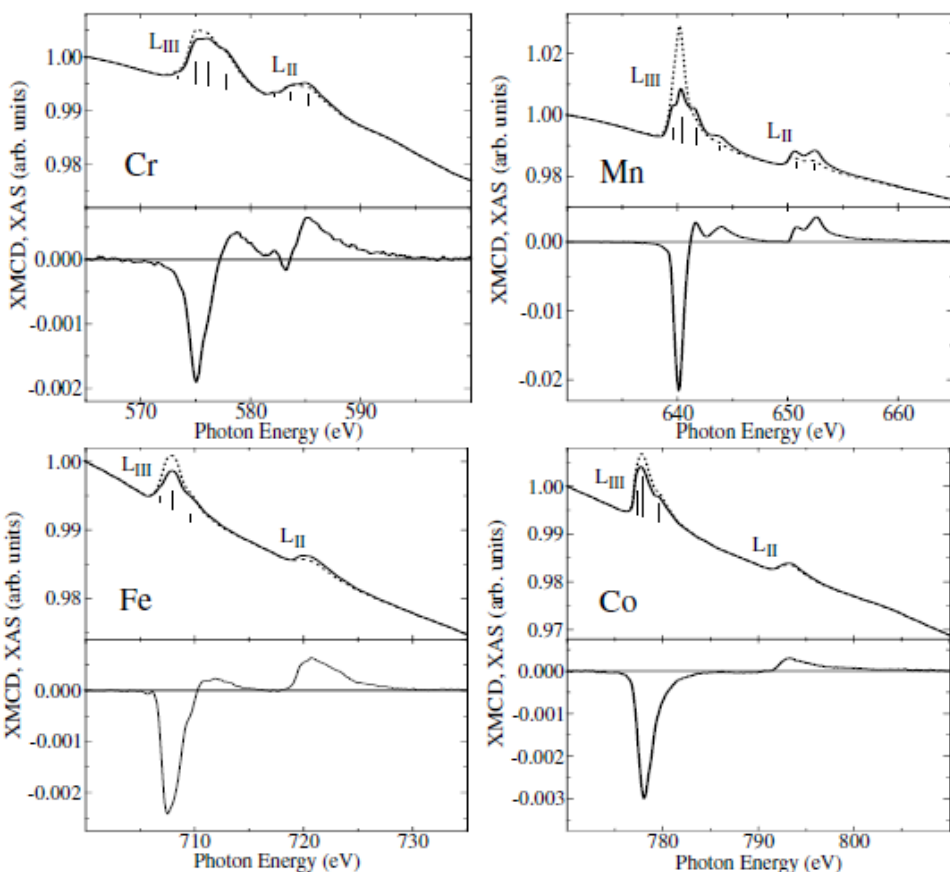
<sup>2</sup>CEA-CNRS, Institut de Chimie de Grenoble, BP 220, F-38043 Grenoble Cedex, France

<sup>3</sup>Departamento de Física, Universidade de São Paulo, CP 66318, 05315-970 São Paulo, São Paulo, Brazil

(Received 20 March 2003; published 11 August 2004)

TABLE I. Experimental values of  $R$  and the derived orbital/spin magnetic moment ratios for 3d impurities in noble metals. The applied field was 7 T, and temperatures  $T$  are in K.

Alloy	$R$	$T$	$\mu_l/\mu_s^{\text{eff}}$
AuCr (1.0 at. %)	-1.01	18.7	-0.003(30)
AuMn (1.0 at. %)	-0.90	6.8	+0.023(20)
CuMn (1.0 at. %)	-0.94	6.8	+0.013(20)
AuFe (0.8 at. %)	-0.86	7.2	+0.034(15)
AuCo (1.5 at. %)	-0.247	6.8	+0.336(52)

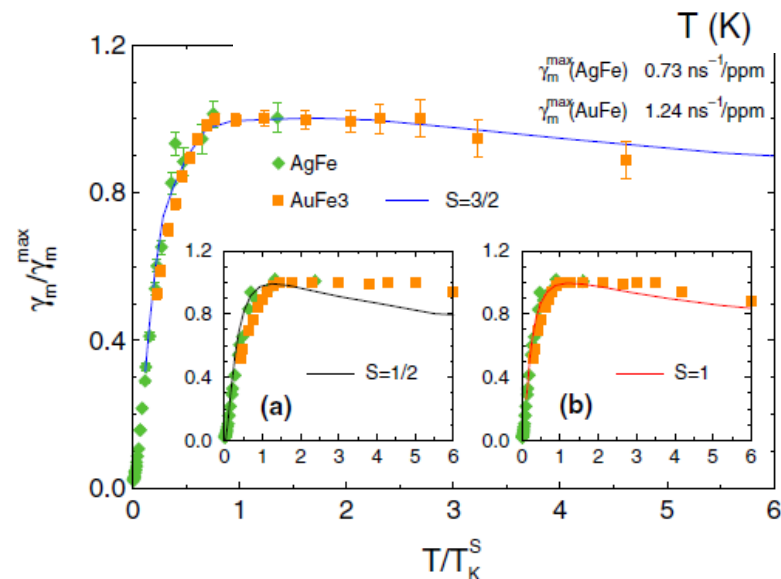
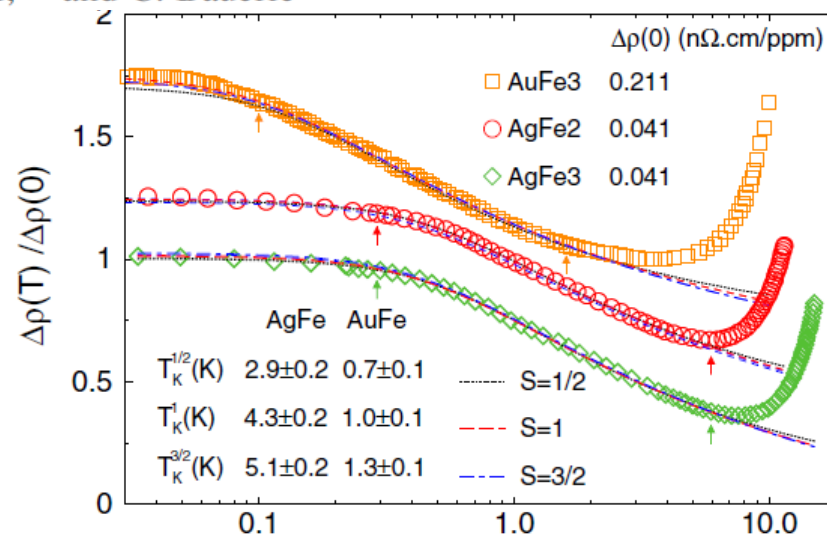
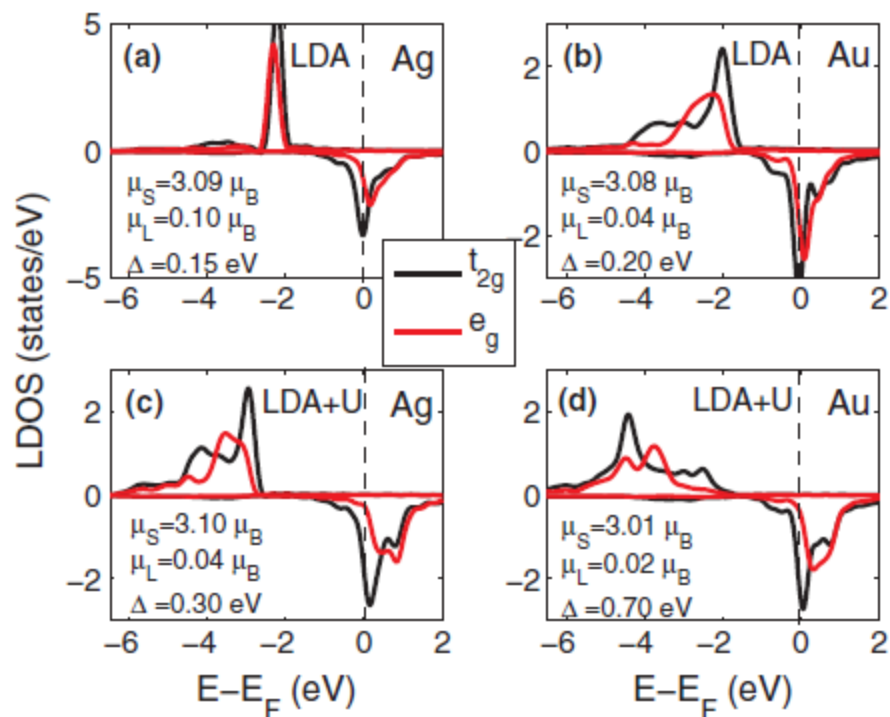


# Kondo Decoherence: Finding the Right Spin Model for Iron Impurities in Gold and Silver

T. A. Costi,<sup>1,2</sup> L. Bergqvist,<sup>1</sup> A. Weichselbaum,<sup>3</sup> J. von Delft,<sup>3</sup> T. Micklitz,<sup>4,7</sup> A. Rosch,<sup>4</sup> P. Mavropoulos,<sup>1,2</sup>  
P. H. Dederichs,<sup>1</sup> F. Mallet,<sup>5</sup> L. Saminadayar,<sup>5,6</sup> and C. Bäuerle<sup>5</sup>

suggests an effective 3-channel  
Kondo model

$$H = \sum_{k\alpha\sigma} \varepsilon_k c_{k\alpha\sigma}^\dagger c_{k\alpha\sigma} + J \sum_{\alpha} \mathbf{S} \cdot \mathbf{s}_{\alpha}.$$



## 2) Quantum Monte Carlo simulation

[Gu, Gan, Bulut, Ziman, Guo, Nagaosa, Maekawa, PRL105 (2010) 086401]

### (1) Single-impurity multi-orbital Anderson Model

A realistic Anderson model is formulated with the host band structure and the impurity-host hybridization determined by ab initio DFT-LDA calculations.

$$H = \sum_{\alpha,k,\sigma} \varepsilon_{\alpha k} c_{\alpha k \sigma}^+ c_{\alpha k \sigma} + \sum_{\xi,\sigma} \varepsilon_{\xi} d_{\xi \sigma}^+ d_{\xi \sigma} + \sum_{\alpha,k,\xi,\sigma} (V_{\alpha k \xi} c_{\alpha k \sigma}^+ d_{\xi \sigma} + h.c.) \\ + U \sum_{\xi} n_{\xi \uparrow} n_{\xi \downarrow} + U' \sum_{\sigma,\sigma'} n_{1\sigma} n_{2\sigma'} - J \sum_{\sigma} n_{1\sigma} n_{2\sigma}$$

For host band structure,  $\alpha = 9$  bands (6s, 6p, 5d orbitals of Au) are included.

For impurity-host hybridization,  $\text{Au}_{26}\text{Fe}$  supercell (3X3X3 primitive FCC cell) is considered.  $\xi = 5$  (3d orbitals of Fe).

For impurity Fe, one  $e_g$  orbital ( $z^2$ ) and one  $t_{2g}$  orbital ( $xz$ ) are considered with the following parameters.

$$U = 5 \text{ eV}, J = 0.9 \text{ eV}, U' = U - 2J = 3.2 \text{ eV}$$

# Impurity-host hybridization for fcc $\text{Au}_{26}\text{Fe}$ (DFT-LDA results)

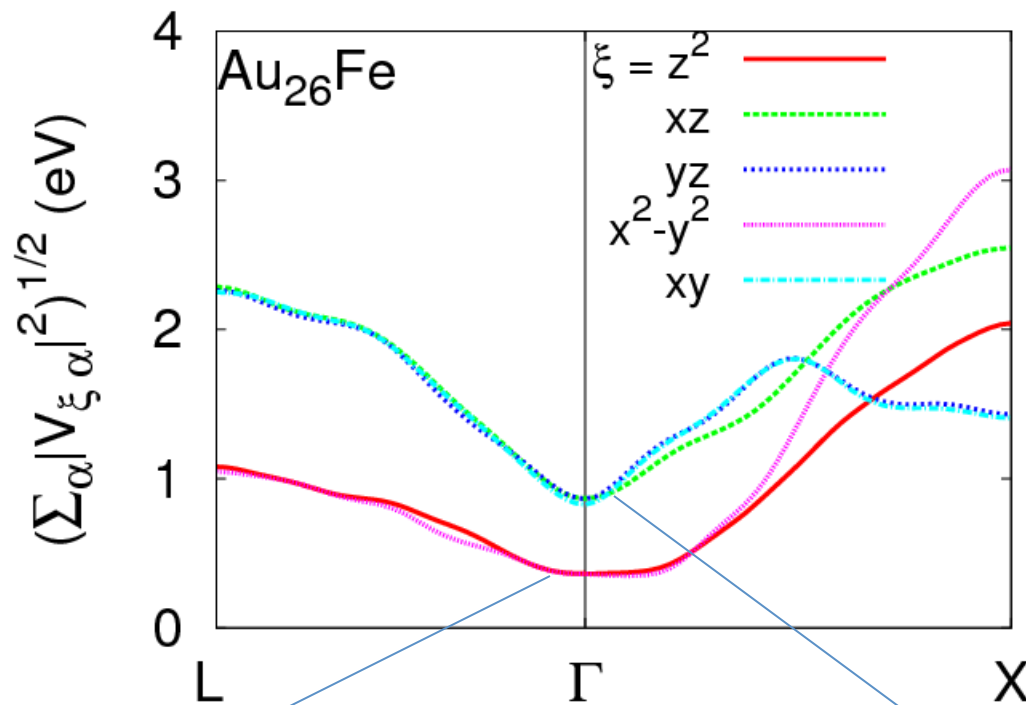
$$\begin{aligned}
 V_{\xi ck} &= \langle \varphi_{\xi} | H_0 | \Psi_{\alpha}(k) \rangle \\
 &= \sum_p a_{cp}(k) \frac{1}{\sqrt{N}} \sum_r e^{ik \cdot r} \langle \varphi_{\xi} | H_0 | \varphi_p(r) \rangle \\
 &= \frac{1}{\sqrt{N}} \sum_{p,r} e^{ik \cdot r} a_{cp}(k) \langle \varphi_{\xi} | H_0 | \varphi_p(r) \rangle
 \end{aligned}$$

For FCC  $\text{Au}_{26}\text{Fe}$  :

$\alpha, p = 9$  (6s, 6p, 5d orbitals of Au)

$r = 26$  ( $\text{Au}_{26}$ )

$\xi = 5$  (3d orbitals of Fe)



□ Energy levels for Fe in  $\text{Au}_{26}\text{Fe}$  (DFT results):

$t_{2g}$  : xz, yz, xy : -0.45 eV

$e_g$  :  $z^2, x^2-y^2$  : -0.55 eV

Smaller mixing for  $e_g$

Larger mixing for  $t_{2g}$



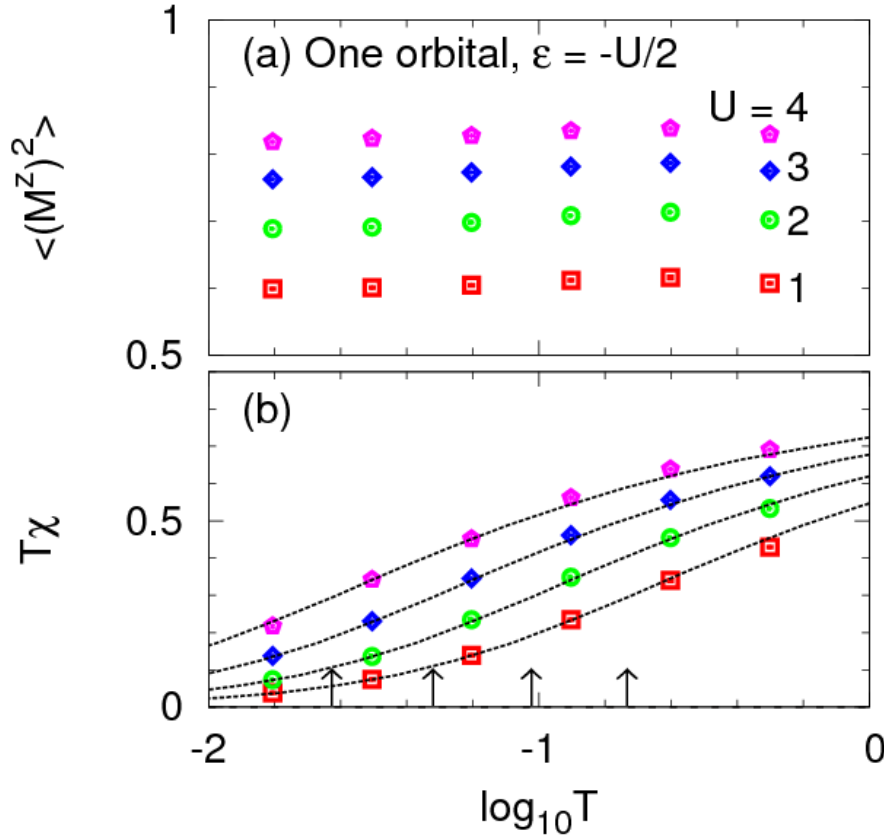
## (2) Magnetic behaviors for Fe in Au from QMC simulations

The magnetic behaviors of the Anderson impurity model at finite temperature are calculated by the Hirsh-Fye quantum Monte Carlo (QMC) technique.

[Hirsch and Fye, PRL 56, 2521(1986)]

Universal Kondo susceptibility for the one orbital case

$\varepsilon_d = -U/2$  (Symmetric case, constant DOS).



$U = 1, 2, 3, 4$  eV  
 $T_K = 0.169, 0.0865, 0.0435, 0.0216$  eV  
 1 eV  $\sim$  10,000 K. 0.0216 eV  $\sim$  200 K

$$J_{sd} = \frac{2V^2U}{\varepsilon_d(\varepsilon_d + U)} = -\frac{8V^2}{U}$$

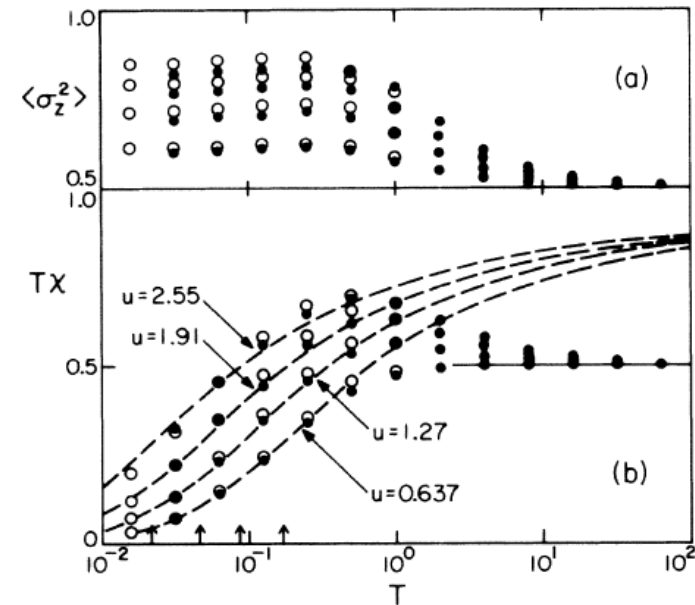


FIG. 2. (a) Local moment  $\langle \sigma_z^2 \rangle$  and (b)  $T\chi$  (spin susceptibility) for a single Anderson impurity;  $\Delta = 0.5$  and  $u = 0.637, 1.27, 1.91, \text{ and } 2.55$ . The closed and open circles correspond to  $\Delta\tau = 0.25$  and  $\Delta\tau = 0.5$ , respectively. The dashed lines are the universal Kondo susceptibility for the four values of  $T_K$  given in the text.

$$u = U/\pi\Delta$$

[Hirsch and Fye, PRL 56, 2521(1986)]

# QMC simulations for Fe in Au

[Gu, Gan, Bulut, Ziman, Guo, Nagaosa, Maekawa, PRL105 (2010) 086401]

## 3-Orbitals case

$$\xi = 1 : z^2,$$

$$\xi = 2 : -\frac{1}{\sqrt{2}}(xz - iyz) : p_1 : l = 1, m = 1;$$

$$\xi = 3 : -\frac{1}{\sqrt{2}}(xz + iyz) : p_{-1} : l = 1, m = -1.$$

## Local moment

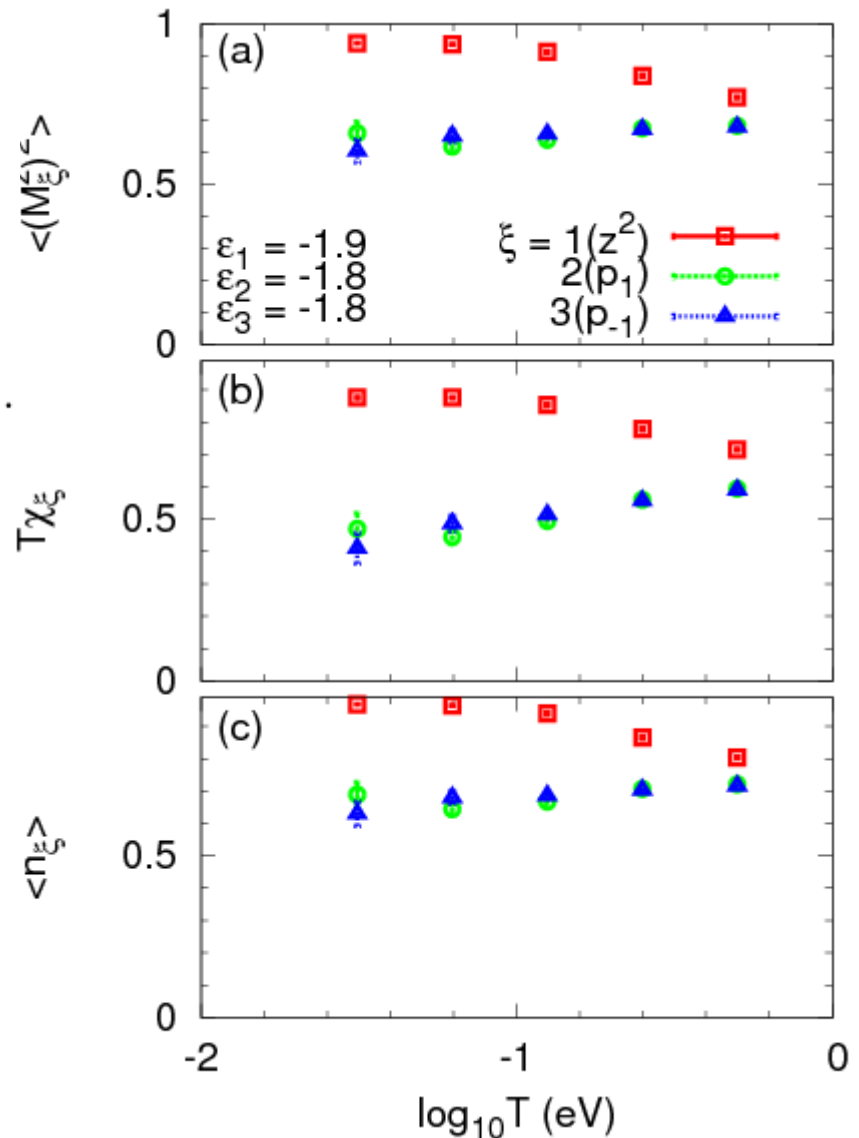
$$M_\xi^z = n_{\xi\uparrow} - n_{\xi\downarrow},$$

## Impurity magnetic susceptibility

$$\chi_\xi = \int_0^\beta d\tau \langle M_\xi^z(\tau) M_\xi^z(0) \rangle,$$

## Occupation number

$$n_\xi = n_{\xi\uparrow} + n_{\xi\downarrow},$$



### (3) Spin-orbit interaction within $t_{2g}$ orbitals for Fe in Au

[Gu, Gan, Bulut, Ziman, Guo, Nagaosa, Maekawa, PRL105 (2010) 086401]

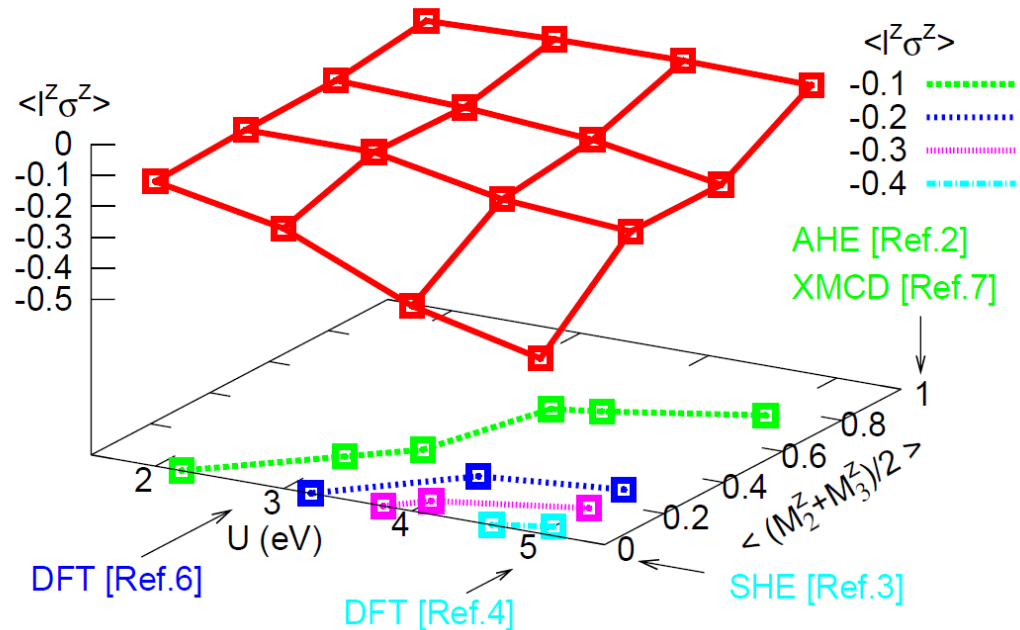
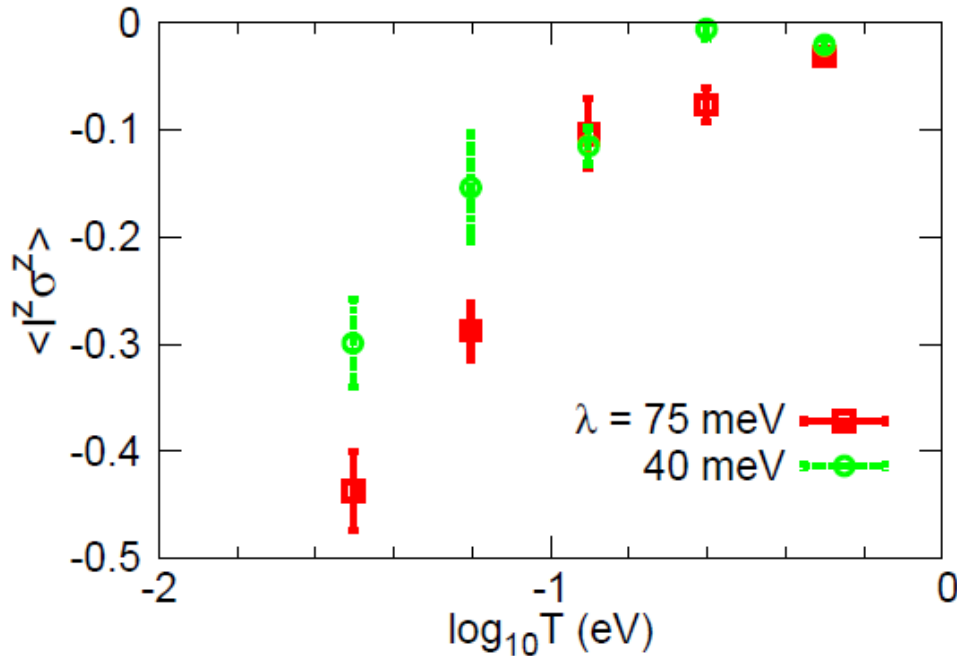
Ising-type spin-orbit interaction for  $p$ -electrons:  $l = 1, m = 1, 0, -1$ .

$$H_{so} = (\lambda/2) \sum_{m,m',\sigma,\sigma'} d_{m\sigma}^\dagger(\mathbf{l})_{mm'} \cdot (\sigma)_{\sigma\sigma'} d_{m'\sigma'}$$

$$l^z = \begin{pmatrix} 1 & 0 & 0 \\ 0 & 0 & 0 \\ 0 & 0 & -1 \end{pmatrix}, \sigma^z = \begin{pmatrix} 1 & 0 \\ 0 & -1 \end{pmatrix},$$

$$H_{so} = (\lambda/2) \sum_{m,\sigma} d_{m\sigma}^\dagger(\mathbf{l})_{mm}^z (\sigma)_{\sigma\sigma}^z d_{m\sigma}$$

$$H_{so} = (\lambda/2) (n_{1\uparrow} - n_{1\downarrow} - n_{-1\uparrow} + n_{-1\downarrow}), \quad T = 350 \text{ K}, = 75 \text{ meV}$$



## (4) Estimation of spin Hall angle for Fe impurity in Au

$$\gamma_s \cong -\frac{3\delta_1(\cos 2\delta_2^+ - \cos 2\delta_2^-)}{9\sin^2 \delta_2^+ + 4\sin^2 \delta_2^- + 3[1 - \cos 2(\delta_2^+ - \delta_2^-)]}$$

Since we consider only two  $t_{2g}$  orbitals with  $\ell_z = \pm 1$ , the SOI within the  $t_{2g}$  orbitals gives rise to the difference in the occupation numbers between the parallel ( $n_P$ ) and anti-parallel ( $n_{AP}$ ) states of the spin and angular momenta. These occupation numbers are related to the phase shifts  $\delta_P$  and  $\delta_{AP}$ , through generalized Friedel sum rule, respectively, as  $n_{P(AP)} = \delta_{P(AP)}/\pi$ , and  $\pi \langle \ell_z \sigma_z \rangle = \delta_P - \delta_{AP}$ ,  $\pi \langle n_2 \rangle = \pi \langle n_3 \rangle = \delta_P + \delta_{AP}$ .

Putting  $\langle \ell_z \sigma_z \rangle = -0.44$  for  $\lambda = 75$  meV, and  $\langle n_2 \rangle = \langle n_3 \rangle = 0.65$ , we obtain  $\delta_P = 1.35$  and  $\delta_{AP} = 2.73$ .

Taking into account the estimate  $\sin \delta_1 \simeq 0.1$ ,  $\gamma_s \simeq 0.06$  is thus obtained.

[Seki, et al., Nat. Mater. 7 (2008)125]

$\gamma_s \simeq 0.11$  (exp.)

# Influence of Fe Impurity on Spin Hall Effect in Au

Isamu Sugai<sup>1</sup>, Seiji Mitani<sup>2</sup>, and Koki Takanashi<sup>1</sup>

<sup>1</sup>Institute for Materials Research, Tohoku University, Sendai 980-8577, Japan

<sup>2</sup>National Institute for Materials Science, Tsukuba 305-0047, Japan

We investigated the influence of Fe impurity on spin Hall effect in Au using multi-terminal devices consisting of an FePt perpendicular spin polarizer and a Au Hall cross with different Fe impurity concentrations. As the Fe impurity concentration was increased in the range of 0–0.95 at. %, the resistivity of Au doped with Fe increased and the spin diffusion length decreased from 35 nm to 27 nm. On the other hand, the spin Hall angle for Au doped with Fe, evaluated from the spin injector-Hall cross distance dependence of spin Hall signals, was approximately 0.07, independent of the Fe concentration. The experimental results provide important information for understanding the mechanism of the large spin Hall effect.

PARAMETERS OF  $P_{\text{AuFe}}$ ,  $R_s^{\text{AuFe}}$ ,  $\lambda_{\text{AuFe}}$ ,  $P$  AND  $\alpha_H$  OBTAINED FOR THE PRESENT FePt/Au DEVICES

Skew scattering

$\gamma_s \sim 0.07$ ,

independent of  
Fe concentration.

	$\rho_{\text{AuFe}}$ [ $\mu\Omega \cdot \text{cm}$ ]	$\lambda_{\text{AuFe}}$ [nm]	$R_s^{\text{AuFe}}$ [ $\Omega$ ]	$P$	$\alpha_H$
Non-doped Au	3.6	$35 \pm 4$	1.1	0.038	$0.07 \pm 0.02$
$\text{Au}_{99.58}\text{Fe}_{0.42}$	4.3	$33 \pm 3$	1.3	0.034	$0.07 \pm 0.01$
$\text{Au}_{99.05}\text{Fe}_{0.95}$	7.0	$27 \pm 3$	1.7	0.027	$0.07 \pm 0.03$

## 5. Open questions

Possible gigantic spin Hall effect in Au due to light impurities of C and N

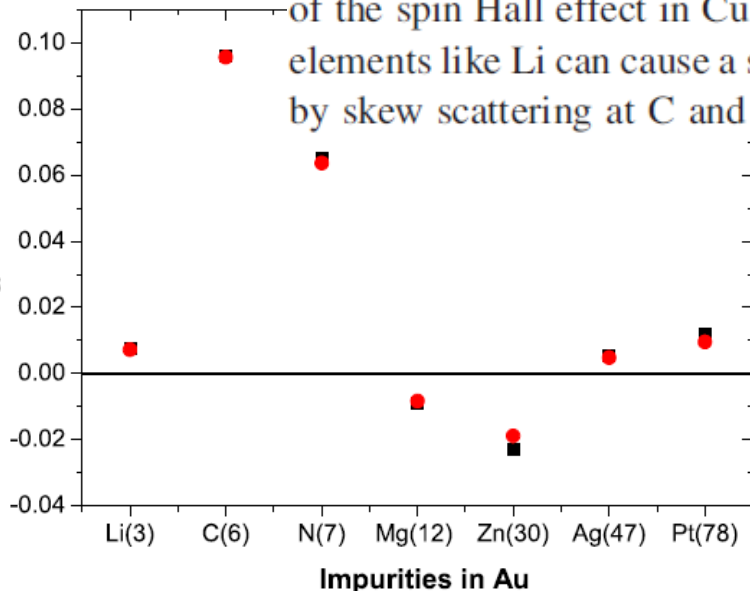
PRL **104**, 186403 (2010)

PHYSICAL REVIEW LETTERS

### Extrinsic Spin Hall Effect from First Principles

Martin Gradhand,<sup>1,2,\*</sup> Dmitry V. Fedorov,<sup>2</sup> Peter Zahn,<sup>2</sup> and Ingrid Mertig<sup>2,1</sup>

We present an *ab initio* description of the spin Hall effect in metals. Our approach is based on density functional theory in the framework of a fully relativistic Korringa-Kohn-Rostoker method and the solution of a linearized Boltzmann equation including the scattering-in term (vertex corrections). The skew scattering mechanism at substitutional impurities is considered. Spin-orbit coupling in the host as well as at the impurity atom and the influence of spin-flip processes are fully taken into account. A sign change of the spin Hall effect in Cu and Au hosts is obtained as a function of the impurity atom, and even light elements like Li can cause a strong effect. It is shown that the *gigantic* spin Hall effect in Au can be caused by skew scattering at C and N impurities which are typical contaminations in a vacuum chamber.



Thus, further careful experiments are needed to clarify the origin of the gigantic SHE in Au/FePt by Seki et al.

## IV. Summary

1. Spin Hall effect, a manifestation of special relativity, is rich of fundamental physics, and also related to such classic phenomena in condensed matter physics as Kondo effect.
2. Spin Hall effect may be used to generate, detect and manipulate spin currents, and hence has important applications in such hot fields as spintronics.
3. *Ab initio* band theoretical calculations not only play an important role in revealing the mechanism of spin Hall effect, but also help in searching for new spintronic materials.

# Acknowledgements:

## Discussions and Collaborations:

Qian Niu (UT Austin), Yugui Yao (BIT)  
Tsung-Wei Chen (Nat'l Taiwan U.)  
Naoto Nagaosa (Tokyo U.)  
Shuichi Murakami (Tokyo Inst. Techno.)  
Bo Gu, Sadamichi Maekawa (Tohoku U.)

## Financial Support:

National Science Council of Taiwan.



## Relativity and spin-orbit interaction

In special relativity, a moving charged particle in an electric field ‘feels’ a ‘magnetic’ field [e.g., Jackson’s textbook]

$$\mathbf{B}' = -\gamma \frac{\mathbf{v}}{c} \times \mathbf{E}; \quad \left( \frac{\mathbf{E} \times \mathbf{p}}{mc} \right)$$

This ‘magnetic’ field would then interact with the spin of the particle (electron)

$$H_{SO} = -\boldsymbol{\mu} \cdot \mathbf{B}' = \frac{(g-1)e}{2mc} \mathbf{s} \cdot \left( \frac{\mathbf{E} \times \mathbf{p}}{mc^2} \right); \quad -\frac{1}{2m^2 c^2} \mathbf{s} \cdot (\nabla V(\mathbf{r}) \times \mathbf{p})$$

For a spherical symmetric atomic potential (e.g., near the nucleus),

$$H_{SO} = -\frac{1}{2m^2 c^2} \mathbf{s} \cdot \left( \frac{dV}{dr} \frac{\mathbf{r}}{r} \times \mathbf{p} \right) = -\frac{1}{2m^2 c^2 r} \frac{dV}{dr} (\mathbf{s} \cdot \mathbf{L}) \approx -\frac{Ze^2}{2m^2 c^2 r^3} (\mathbf{s} \cdot \mathbf{L})$$

# Outlook

Most activities in the field are currently focused on quantum spin Hall effect and topological insulators.

Zoo of the Hall Effects:

Ordinary Hall effect (Hall 1879);

Anomalous Hall effect (Hall 1880 & 1881);

▲ Extrinsic spin Hall effect (Dyakonov & Perel 1971);

Integer quantum Hall effect (von Klitzing et al. 1980);

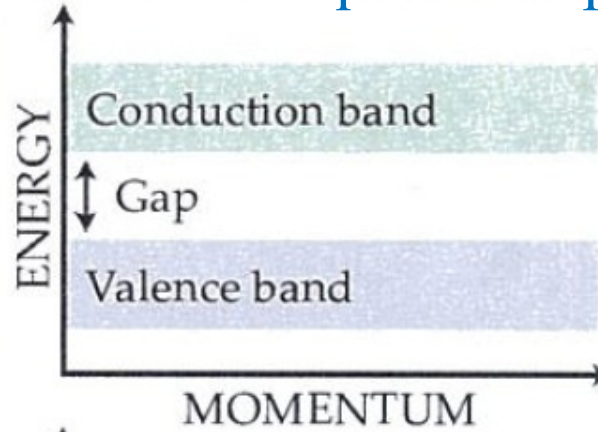
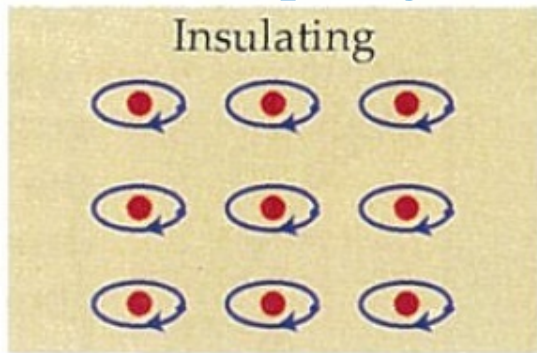
Fractional quantum Hall effect (Tsui et al. 1982);

▲ Intrinsic spin Hall effect (Murakami et al. 2003; Sinova et al. 2004).

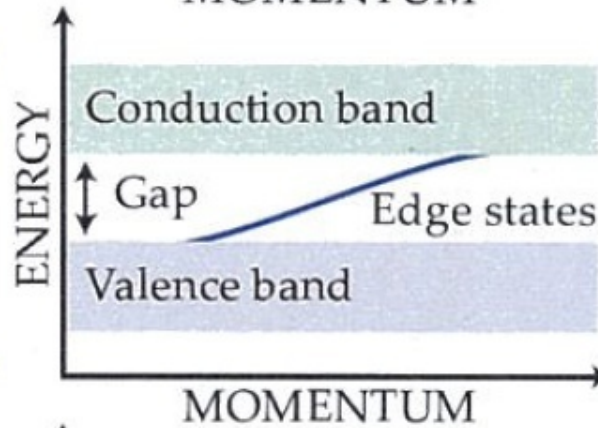
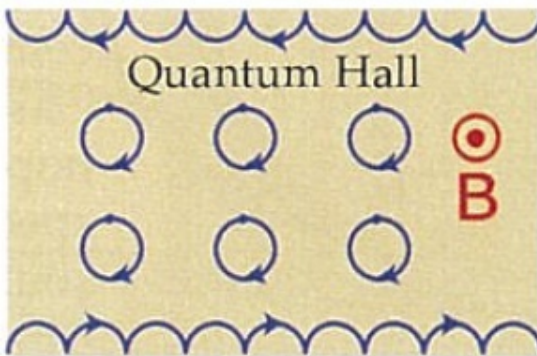
➔ Quantum spin Hall effect (Kane & Mele 2005, Bernevig & Zhang 2006)

Quantized anomalous Hall effect (Xue et al. 2013)

# Topological insulators & quantum spin Hall effect

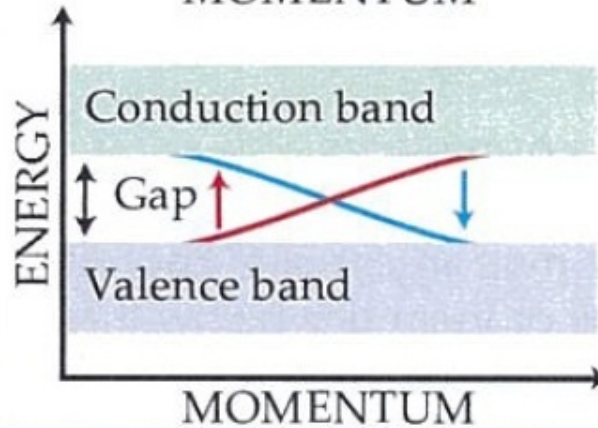
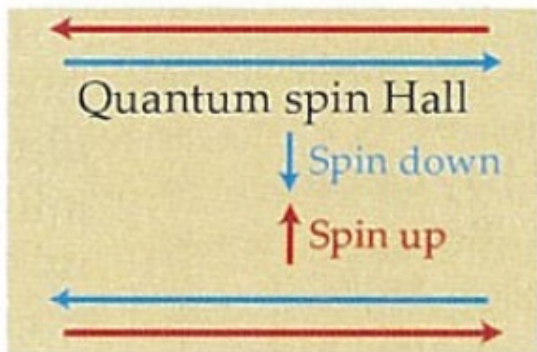


Ordinary insulators  
Band gap, localization gap etc



Quantum Hall insulators  
Gap due to Landau level formation induced by applied magnetic field

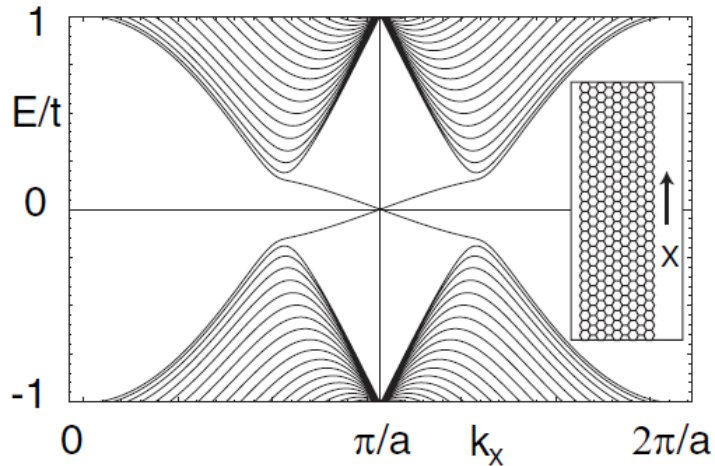
Topological invariant: Chern number



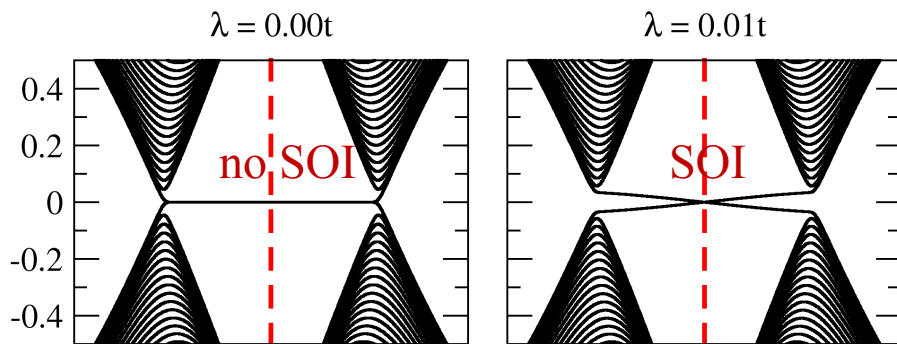
Topological insulators  
Nonzero topological invariant  $Z_2$ :  
Edge states: time reversal symmetry

## (i) Zigzag graphene strips as 2D topological insulators

[Kane & Mele, PRL 2005]

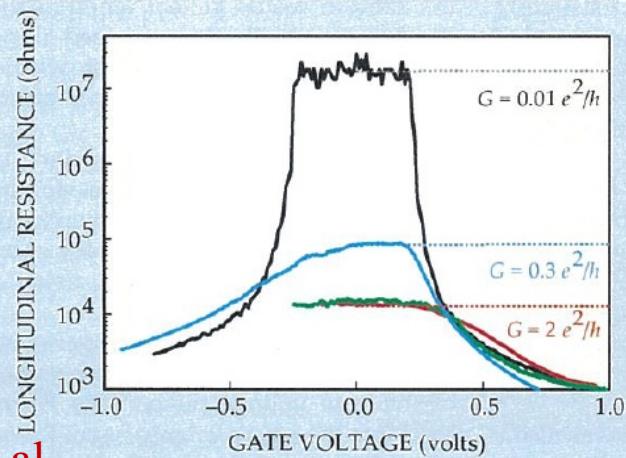


[Chen, Xiao, Chiou, Guo PRB 2011]



SOI is too small ( $< 0.01$  meV) to make QSHE observable!

[Koenig et al. Sci 2007]

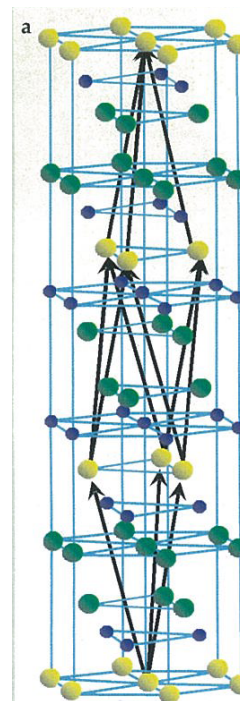


Fermi level lies in the bandgap, resistance is high. The red, green, and blue traces come from samples whose thickness ( $d > 6.3$  nm) ensures that they can carry edge states. Quantization of the conductance  $G$  is observed when the sample is shorter than the electrons' mean free path. That's the case for the red and green traces but not for the blue trace. (Adapted from ref. 5.)

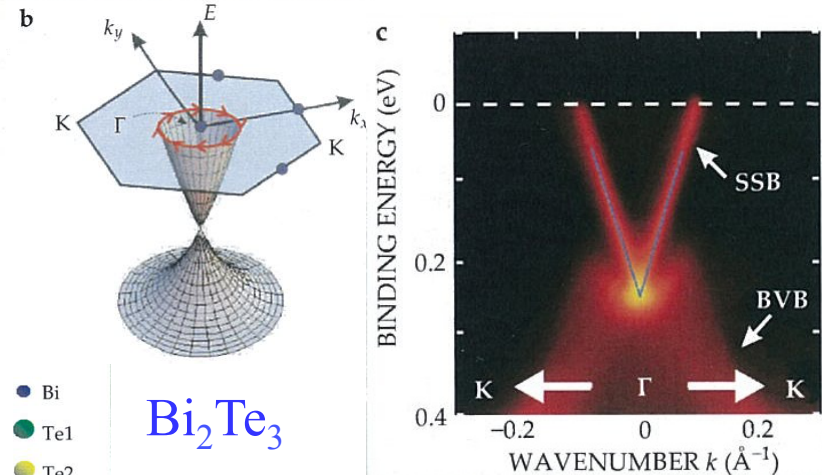
**Figure 3.** The quantum spin Hall effect features quantized edge currents. To be sure of seeing them, the Würzburg group gated their device to sweep the Fermi level from the valence band, through the bandgap, and into the conduction band. The black trace comes from a sample whose thickness ( $d < 6.3$  nm) ensures that it behaves like a normal insulator. When the

## (ii) Natural semiconductors as 3D topological insulators

[Bernevig Hughes, Zhang, Sci. 2006]



$\text{Bi}_2\text{Te}_3$



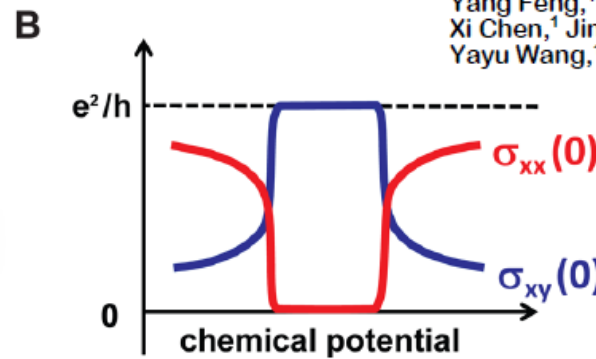
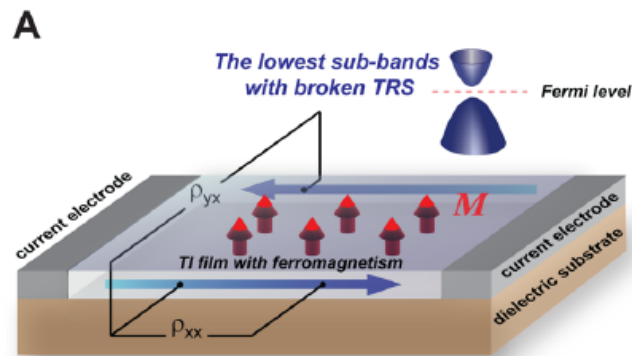
[Chen et al. Science 2009]

## (iii) Quantized anomalous Hall effect in magnetic topological insulators

[Xue et al. Sci 2013/3/31]

### Experimental Observation of the Quantum Anomalous Hall Effect in a Magnetic Topological Insulator

Cui-Zu Chang,<sup>1,2\*</sup> Jinsong Zhang,<sup>1\*</sup> Xiao Feng,<sup>1,2\*</sup> Jie Shen,<sup>2\*</sup> Zuocheng Zhang,<sup>1</sup> Minghua Guo,<sup>1</sup> Kang Li,<sup>2</sup> Yunbo Ou,<sup>2</sup> Pang Wei,<sup>2</sup> Li-Li Wang,<sup>2</sup> Zhong-Qing Ji,<sup>2</sup> Yang Feng,<sup>1</sup> Shuaihua Ji,<sup>1</sup> Xi Chen,<sup>1</sup> Jinfeng Jia,<sup>1</sup> Xi Dai,<sup>2</sup> Zhong Fang,<sup>2</sup> Shou-Cheng Zhang,<sup>3</sup> Ke He,<sup>2†</sup> Yayu Wang,<sup>1†</sup> Li Lu,<sup>2</sup> Xu-Cun Ma,<sup>2</sup> Qi-Kun Xue<sup>1,2†</sup>



observed in  $\text{Cr}_{0.15}(\text{Bi}_{0.1}\text{Sb}_{0.9})_{1.85}\text{Te}_3$  film

